NUCLEAR DATA AND MEASUREMENTS SERIES

ANL/NDM-16

Fast Neutron Excitation of the Ground-State Rotational Band of ^{238}U

by

P. Guenther, D. Havel, and A. Smith

September 1975

ARGONNE NATIONAL LABORATORY,
ARGONNE, ILLINOIS 60439, U.S.A.

NUCLEAR DATA AND MEASUREMENTS SERIES

ANL/NDM-16

Fast Neutron Excitation of the Ground-State Rotational Band of ^{238}U

by

P. Guenther, D. Havel and A. Smith

September 1975

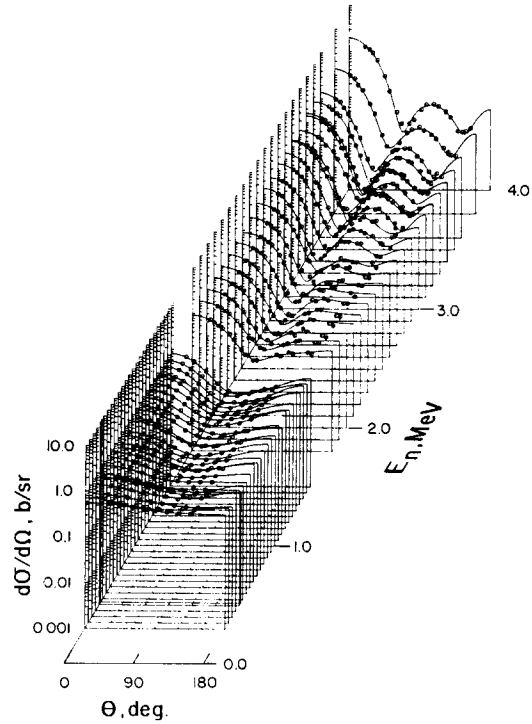

U of C - AUA - USAEC

ARGONNE NATIONAL LABORATORY,
ARGONNE, ILLINOIS 60439, U.S.A.

The facilities of Argonne National Laboratory are owned by the United States Government. Under the terms of a contract (W-31-109-Eng-38) between the U. S. Atomic Energy Commission, Argonne Universities Association and The University of Chicago, the University employs the staff and operates the Laboratory in accordance with policies and programs formulated, approved and reviewed by the Association.

MEMBERS OF ARGONNE UNIVERSITIES ASSOCIATION

The University of Arizona
Carnegie-Mellon University
Case Western Reserve University
The University of Chicago
University of Cincinnati
Illinois Institute of Technology
University of Illinois
Indiana University
Iowa State University
The University of Iowa
Kansas State University
The University of Kansas
Loyola University
Marquette University
Michigan State University
The University of Michigan
University of Minnesota
University of Missouri
Northwestern University
University of Notre Dame
The Ohio State University
Ohio University
The Pennsylvania State University
Purdue University
Saint Louis University
Southern Illinois University
The University of Texas at Austin
Washington University
Wayne State University
The University of Wisconsin

NOTICE

This report was prepared as an account of work sponsored by the United States Government. Neither the United States nor the United States Atomic Energy Commission, nor any of their employees, nor any of their contractors, subcontractors, or their employees, makes any warranty, express or implied, or assumes any legal liability or responsibility for the accuracy, completeness or usefulness of any information, apparatus, product or process disclosed, or represents that its use would not infringe privately-owned rights.

ANL/NDM-16

Fast Neutron Excitation of the Ground-State Rotational Band of ^{238}U

by

P. Guenther, D. Havel and A. Smith

September 1975

In January 1975, the research and development functions of the former U.S. Atomic Energy Commission were incorporated into those of the U.S. Energy Research and Development Administration.

Applied Physics Division
Argonne National Laboratory
9700 South Cass Avenue
Argonne, Illinois 60439
U.S.A.

NUCLEAR DATA AND MEASUREMENTS SERIES

The Nuclear Data and Measurements series presents results of studies in the field of microscopic nuclear data. The primary objective is the dissemination of information in the comprehensive form required for nuclear technology applications. This Series is devoted to: a) Measured microscopic nuclear parameters, b) Experimental techniques and facilities employed in data measurements, c) The evaluation of nuclear data. Contributions to this Series are reviewed to assure technical competence and, unless otherwise stated, the contents can be formally referenced. This Series does not supplant formal journal publication but it does provide the more extensive information required for technological applications (e.g., tabulated numerical data) in a timely manner.

TABLE OF CONTENTS

Fast Neutron Excitation of the Ground-State Rotational Band of ^{238}U*

by

P. Guenther, D. Havel and A. Smith

Argonne National Laboratory
Argonne, Illinois 60439

ABSTRACT

The differential neutron cross sections for the excitation of the 2+(45 keV), 4+(148 keV) and 6+(308 keV) states of ^{238}U are measured for scattered neutron energies in the range 0.1 to 3.0 MeV. The observed excitation cross sections vary smoothly with energy with no significant fluctuations. The experimental results are correlated with the predictions of compound-nucleus and direct-reaction models. At lower energies ($\lesssim$ 0.8 MeV) the observed inelastic scattering cross sections are consistent in shape and magnitude with the predictions of compound-nucleus theory. Above $\gtrsim$ 1.0 MeV comparison of measured and calculated values indicates large direct-reaction contributions. The experimental and computational results are compared with the evaluated nuclear data file, ENDF/B-IV, and significant discrepancies are noted. The present results and selected values from the literature are used to deduce an evaluated set of ^{238}U inelastic scattering cross sections.

*This work supported by the U.S. Energy Research and Development Administration.

I. INTRODUCTION

Over nearly two decades a number of experimental studies of the neutron excitation of the ground-state rotational band of ^{238}U have been reported (1-7). These measurements indicate that the cross sections for the excitation of the first 2+(45 keV) state are large at incident neutron energies of less than 1.0 MeV. However, the experimental cross sections become uncertain as the threshold for the reaction is approached with discrepancies as much as a factor of two between measured values in both shape and magnitude. Recent measurements with improved experimental resolutions indicate that the cross sections for the excitation of this first state remain large into the several MeV range (6,7). The cross sections for the excitation of the second state 4+(148 keV) have been measured to energies of greater than 1.5 MeV with reasonably consistent results. The excitation of the third state 6+(308 keV) has been qualitatively observed but the corresponding cross sections are small and uncertain. The neutron cross sections for the excitation of the higher-energy states of the first-rotational band have apparently not been quantitatively measured.

Theoretical interpretations of the above experimental results have been reported by a number of authors (6-18). ^{238}U is a statically-deformed rotational nucleus and substantial direct excitation of the collective states by few MeV neutrons can be expected. Some recent experimental results bear-out this expectation (6,7). At energies of less than 1.0 MeV the inelastic neutron scattering should consist primarily of the compound-nucleus component. A number of calculations based upon this assumption have resulted in inelastic neutron scattering cross sections that differ in both shape and magnitude from some of the experimental values (10). Corrections to the compound-

nucleus results attributed to: width fluctuations, correlation enhancement and a direct-reaction component have not generally resolved these calculational-experimental discrepancies. In addition, some of the measured values indicate a fluctuating structure in the lower energy cross sections that has not been explained theoretically. Generally, some major changes at lower energies in some experimental results and/or theory are indicated in order to make the two relatively consistent.

The resolution of the above experimental and/or theoretical uncertainties is of considerable applied importance. The inelastic neutron scattering cross sections of ^{238}U have a direct impact on the neutronic design of fast fission reactors, particularly at lower (e.g., less than 1.0 MeV) neutron energies. More generally, the ^{238}U neutron inelastic scattering cross sections should be similar to those of a number of actinides appearing with abundance in fission-based energy systems (e.g., ^{240}Pu). Experimental measurements of the scattering cross sections of many of these actinides is very difficult and thus a capability for reliable theoretical prediction is of considerable applied importance.

The present studies had the objectives of: 1) providing improved experimental definition of the low-(less than 600 keV) and high-(greater than 1.5 MeV) energy cross sections for the excitation of the ground-state rotational band of ^{238}U, 2) a verification of previously reported experimental values in the energy range 0.4 to 1.5 MeV, 3) a quantitative theoretical interpretation of the experimental results including both compound- and direct-reaction mechanisms, and 4) the provision of the experimental and theoretical results in the form of an evaluated data set suitable for applied use. The following portions of this paper consist of: an outline of the experimental methods (Sec.II), the experimental results (Sec. III), comparisons with

previously reported experimental values (Sec. IV), a physical interpretation of the measured quantities (Sec. V), and the formulation of the evaluated data set (Sec. VI). The numerical values of the evaluated data set are given in the Appendix in the ENDF/B format (19).

II. EXPERIMENTAL METHODS

Two sample configurations were employed in the measurements. Most of the measurements in the incident neutron energy range 0.4 to 3.0 MeV and all of the angular distribution measurements employed solid cylindrical samples of natural uranium 2 cm long and 2 cm in diameter with neutrons incident upon their lateral surfaces. Many of the measurements in the incident neutron energy range 0.1 to 0.6 MeV employed square uranium-plate samples 5 cm on a side and 1.2 cm thick oriented at a 45 deg. angle with respect to the axis of the incident neutron beam. All cross sections are reported as barns-per-atom of the natural element. Corrections for the small ^{235}U content would generally have been far less than the uncertainties associated with the experimental measurements. Standard reference samples of carbon and polyethylene were used in the same geometries as the uranium samples.

The $^{7}Li(p,n)^{7}Be$ reaction was employed as a neutron source throughout the measurements (20). Lithium metal films were deposited upon tantalum backing plates to sufficient thicknesses to provide incident neutron energy spreads at the scattering samples of approximately 10 to 20 keV.

The measurements were made using fast time-of-flight techniques. The majority of the measurements utilized the Argonne National Laboratory Tandem Dynamitron. This facility provided an essentially monoenergetic proton burst at repetition rates varying from 1 to 2 MHz (21). The burst duration was nominally 1 nsec with a minimum of

800 to 900 psec for measurements demanding of the optimum resolutions. These burst durations were estimated by observing the gamma-ray from the source reaction and included uncertainties due to gamma-ray detection and time analysis. The scattering samples were placed 13 to 15 cm from the source at a zero deg. reaction angle. The flight path was defined by a massive collimator system. The neutron detectors were proton-recoil scintillators of various sizes and configurations chosen to optimize the time resolution and sensitivity in the various experimental energy intervals. The details of the apparatuses and method have been described extensively elsewhere (22,23).

All uranium and reference-standard measurements were corrected for multiple scattering, incident beam attenuation and angular-resolution effects using a combination of analytical and Monte-Carlo computational procedures (24,25). Some of the corrections were large and considerable care was taken to assure their validity. The Monte-Carlo calculations were carried to statistical accuracies far smaller than the experimental uncertainties (e.g., to less than 1 percent uncertainty). The corrected results obtained with samples of widely differing masses were consistent.

At incident neutron energies of less than 1.5 MeV the ^{238}U cross sections were determined relative to the standard-reference carbon cross sections. The carbon reference cross sections were constructed from the carbon total cross sections as given in ENDF/B-IV, MAT-1274, (19) and from the angular distributions as given by Langsdorf et al. (26). Most of the carbon calibrations at energies below 600 keV were made at a scattering angle of 90 deg. using the cross section given by

$$\frac{d\sigma}{d\Omega} = \frac{\sigma_t}{4\pi} \left(1 - \frac{W_2}{2}\right) \qquad (1)$$

Since the W_2 is less than 0.1 in this energy range, the reference 90-deg. carbon cross sections were not particularly sensitive to uncertainties in the carbon angular distributions (i.e., to relatively large uncertainties in the W_2 value). The uncertainty in the carbon total cross section was estimated to be less than 2 percent in this energy range and that of the 90-deg. differential cross sections less than 3 percent. Over the energy range 0.6 to 1.5 MeV the carbon calibrations were based upon the differential cross sections of Langsdorf et al. (26). The estimated uncertainties in the calibration in this energy range were 5 to 8 percent. At incident neutron energies of 1.5 MeV and above the ^{238}U cross sections were determined relative to the well known H(n,n) cross sections (27) using the experimental methods defined in Refs. 22 and 23.

III. EXPERIMENTAL RESULTS

The experimental results were obtained in four Data Sets. Data Set-1 extended from scattered neutron energies of 100 to 600 keV with the objective of defining the inelastic scattering cross section to be near threshold as possible. Data Set-2 was confined to an incident neutron energy of 550 keV with the objective of a good definition of the inelastic scattering cross section magnitude and angular distribution at this single and experimentally favorable energy. Data Set-3 extended from 400 to 1200 keV with the intent of verifying previously reported inelastic scattering cross sections in this region, particularly the excitation of the 4+(148 keV) and 6+(308 keV) states. Data Set-4 extended from 1.5 to 3.0 MeV with attention to the resolution of the cross sections for the excitation of the first two excited states (2+, 45 keV and 4+, 148 keV) in a region where direct reaction processes are expected to be large. Throughout the work

the emphasis was on cross section magnitudes. The observed excitation energies were consistent with those reported in Ref. 28 but the latter are very likely more precise.

A. Data Set-1

These measurements determined the differential cross sections for the inelastic neutron excitation of the 2+(45 keV) state of ^{238}U at a scattering angle of 90 deg. for scattered neutron energies in the range 100 to 600 keV. The measurements employed the slab samples outlined above. The cross sections were determined relative to the 90 deg. scattering cross sections of carbon using a similar slab sample of carbon. In making the carbon calibrations the incident neutron energies were varied so that the neutrons scattered from the carbon had essentially the same energy as those resulting from the excitation of the 45 keV state of ^{238}U. This procedure largely avoided uncertainties due to the relative energy-dependent sensitivities of the detectors. The neutron-source intensity was monitored using four long counters arranged so as to be insensitive to small changes in the neutron-source energy (29). Scattered-neutron flight paths were varied between 2 and 6 meters so as to give the best compromise of resolution, signal-to-background ratio and statistical accuracy. At scattered neutron energies above approximately 200 keV the elastic and inelastic (2+, 45 keV) neutron groups were well resolved as indicated by the time distribution shown in Fig. 1. At lower scattered neutron energies the definition was less satisfactory and graphical procedures assisted in the resolution of the two components guided by response functions determined from the observation of neutrons scattered from carbon and/or lead.

The measured results were corrected for multiple scattering, beam attenuation and angular resolution as outlined above. The samples were large with correspondingly large

corrections (20 to 30 percent). The correction procedures were carefully tested using two different computational systems. However, there was an uncertainty in the application of the corrections to the carbon-reference measurements. The neutron energy degradation in the large carbon samples was considerable and thus some of the multiple-scattered neutrons were detected at energies appreciably different from those of the single-scattered events and with a different detector efficiency. The detector efficiency changed relatively slowly with energy above approximately 250 keV but at lower energies the change was very rapid. The effective resolutions used in the correction calculations were chosen to be similar to those of the particular experimental measurement in order to keep the correction calculations a close analog of the actual experimental measurement. Using this procedure it was estimated that the uncertainties due to the correction factors were less than 5 percent at energies below 250 keV and smaller at higher energies. It was encouraging to note that the corrected results of the slab measurements were consistent with the 550 keV results obtained with the much smaller cylindrical samples (see the discussion of Data Set-2, below).

The Data Set-1 results are given in Table 1 as ratios to the 90 deg. carbon cross sections, as differential 90 deg. ^{238}U cross sections and as angle-integrated cross section values. The latter were obtained from the 90 deg. differential values using the experimentally and the theoretically based angular distributions described in Sec. V. In this energy range the correction for anisotropy was approximately 8±3 percent. The angle-integrated experimental results are summarized and compared with those of Data Set-2 in Fig. 2.

B. Data Set-2

This Data Set was confined to the single incident

neutron energy of 550 keV and had the objective of a precise determination of the 90 deg. differential cross section for the excitation of the 2+(45 keV) state and of the relative determination of the angular dependence of the elastic and of the inelastic (45 keV) scattering cross sections. The measurements employed the smaller cylindrical samples, noted above, and a flight path of 5.7 meters. The experimental resolutions were sufficient to resolve the elastic and inelastic scattered-neutron groups at all measured angles as illustrated by the examples of Fig. 3. Neutron-source intensity was monitored using long counters and a secondary time-of-flight system arranged so as to be insensitive to the angular placement of the primary detector.

The differential 90 deg. inelastic-scattering cross sections were redundantly determined relative to carbon in the same manner as employed in Data Set-1, above. Five independent measurements were made with somewhat different experimental arrangements (e.g., detector sensitivities). The results are summarized in Table 1. The uncertainties of the individual differential measurements were in the range 7 to 9 percent. The average differential 90 deg. cross section for the excitation of the 45 keV state was 0.139 b/sr (± 4 percent). These values and uncertainties include corrections for multiple scattering, beam attenuation and angular resolution carried out as outlined above. The magnitudes of the corrections were approximately 12 to 15 percent depending upon the details of the measurements. The corrections were believed known to 10 percent (i.e., 1 to 1.5 percent in cross section). The average of the 90 deg. values of this Data Set were consistent with the results of Data Set-1 as illustrated in Fig. 2.

The relative angular dependences of the elastic and the inelastic (45 keV) scattering cross sections were determined by measurements at laboratory scattering angles

of approximately 30, 45, 60, 75, 90, 105, 120, 135 and 150 deg. The statistical accuracies of the individual differential values were in the range 5 to 9 percent. The observed relative distributions were least-squares fitted with a Legendre polynomial series from which the relative angle-integrated scattering cross sections were deduced. The inelastic-scattering cross sections were normalized to the measured 90 deg. value discussed above. The normalization of the elastic scattering cross sections was determined from the difference between the known total neutron cross section (8.28 b as given in Ref. 10) and the measured 2+(45 keV) and 4+ (148 keV) inelastic scattering cross sections. An additional small correction was made for the contribution of radiative capture. All of the differential distributions were corrected for multiple scattering, beam attenuation and angular resolution as described above. The angle-integrated 550 keV cross section for elastic scattering derived in this manner was 6.27±0.2 b. The angle-integrated cross section for the excitation of the 2+(45 keV) state by 550 keV neutrons was 1.606±0.065 b excluding the uncertainties associated with the extrapolation of the measured values over the full angular range 0 to 180 deg. The normalized differential values and the associated Legendre polynomial fits to the data are illustrated in Fig. 4.

C. Data Set-3

These measurements extended over the incident neutron energy range 400 to 1200 keV. The primary emphasis was on the inelastic neutron excitation of the 4+ (148 keV) and 6+(308 keV) states of ^{238}U. Secondary attention was given to the excitation of the 2+(45 keV) state with the intent of verifying previously reported

results. The measurements of this Data Set pre-dated those of the other three sets by several years and employed different apparatuses. The experimental apparatuses and methods were essentially identical to those of Ref. 22. The smaller cylindrical samples were used. The flight paths were in the range 2 to 3 meters and, as a consequence, the resolution of the 2+(45 keV) was not generally as satisfactory as that obtained in the newer three sets of measurements. All cross sections were determined relative to those of carbon in the manner previously described (22), and all measured results were corrected for experimental perturbations in a manner similar to that applied to the newer data sets.

The differential inelastic scattering cross sections were determined at up to eight scattering angles distributed between 30 and 150 deg. The angle-integrated inelastic cross sections were deduced from the differential quantities by least-square fitting a Legendre polynomial series to a minimum of four differential values at a given energy. The estimated uncertainties associated with the angle-integrated values varied from less than 10 percent to 50 percent or more depending upon the particular cross sections and incident energies. The uncertainty estimates included contributions from counting statistics and estimated effects of experimental resolutions and detector calibrations. The cross sections for the excitation of the 6+(306 keV) state were small and relatively the most uncertain. The resolution of scattered neutrons due to the excitation of the 2+(45 keV) state was incomplete, particularly at the higher incident energies. This lack of definition increased the uncertainty of these results. In addition, the calibration of the detection system at low energies (400 to 500 keV) lacked reliability, and results in this energy region remain uncertain.

The numerical angle-integrated inelastic cross section results are given in Table 2 and are compared with the 45 keV and 148 keV values obtained in the newer Data Sets in Fig. 5.

D. Data Set-4

This Data Set gave primary attention to cross sections for the excitation of the 2+(45 keV) state and secondary attention to the excitation of the 4+(148 keV) and 6+(308 keV) states in the incident neutron energy range 1.5 to 3.0 MeV. The essential experimental problem was the resolution of the 2+(45 keV) component from the elastic contribution. This problem was particularly severe at forward scattering angles (e.g., 30 deg.) where the elastic contribution was greater by more than an order of magnitude than the inelastic component. The forward-angle inelastic component could not generally be experimentally resolved at incident neutron energies in the several MeV range. Therefore the experiments determined the differential inelastic scattering cross sections at selected and experimentally-favorable large-scattering angles and theory was used to deduce the angle-integrated cross sections from these measured values. The validity of this theoretical extrapolation was verified by complimentary experimental studies of the similarly deformed nucleus ^{186}W. ^{186}W is an experimentally favorable nucleus since its first-excited (2+) state is at 122 keV, nearly three times the energy of the comparable ^{238}U state (28). The differential elastic and inelastic scattering cross sections of ^{186}W were well resolved over a wide angular range to energies of 3.0 MeV thereby providing a good basis for the development of a model suitable for the extrapolation of the more-difficult-to-obtain ^{238}U experimental values. The derivation of this model is outlined in Sec. V, below and discussed in detail in Ref. 30. The suitability

of the model in the context of ^{238}U was verified by comparison of calculated and measured composite differential cross sections for elastic and inelastic (45 keV) scattering. These composite differential ^{238}U measurements were an inherent part of the experimental program and essential to the interpretation and calibration of the inelastic scattering results at incident energies above 1.5 MeV.

The differential cross sections for the composite elastic and inelastic (45 keV) scattering from ^{238}U and the elastic and the inelastic scattering from ^{186}W were measured at 20 or more scattering angles distributed between approximately 20 and 150 deg. and at incident neutron energy intervals of 0.3 MeV from 1.5 to 3.0 MeV. The measurements were made using the multi-angle time-of-flight system and associated methods described in Refs. 22 and 23. The scattering samples were the 2 cm in diameter and 2 cm long cylinders. Flight paths were approximately 5.5 meters. All cross sections were determined relative to the H(n,n) cross section and corrected for multiple scattering, beam attenuation and angular resolution as outlined above. Neutrons due to the excitation of the 2+ (122 keV) state of ^{186}W were well resolved from the elastically scattered neutrons as illustrated by the time distribution of Fig. 6. The relative intensities of the two neutron groups were obtained by least-square fitting the observed time spectra with two Gaussian distributions. These were descriptive of the measured values as illustrated by the curves of Fig. 6 and the relative intensities obtained with the fitting procedures were consistent with those obtained using subjective graphical procedures. The resulting differential elastic and inelastic (2+, 122 keV) scattering cross sections of ^{186}W are illustrated in Fig. 7 and discussed in detail in Ref. 30. These ^{186}W distributions were a foundation for the theoretical model,

discussed in Sec. V, subsequently used for the extrapolation of the ^{238}U measurements. The differential cross sections for the composite elastic and inelastic (2+, 45 keV) scattering from ^{238}U were determined concurrently with the ^{186}W scattering cross sections at similar scattering angles. The methods of normalization and correction were identical with the addition of a small correction for fission neutron contamination. The ^{238}U results are summarized in Fig. 8. The uncertainties associated with these ^{238}U cross sections were generally in the range 5 to 10 percent including contributions from counting statistics, correction factors, and normalization procedures. A more detailed discussion of these uncertainties is given in Ref. 30. Generally, the consistency of the data was in accord with the estimated uncertainties and the carbon cross sections determined concurrently with the ^{238}U and ^{186}W values were in good agreement with those reported in the literature (31). The above ^{238}U angular distributions served as a "benchmark" for testing the model subsequently used for extrapolating the measured ^{238}U inelastic cross section results. The distributions were also essential to the normalization of the differential inelastic scattering results as described in the following paragraphs.

The neutrons inelastically scattered from ^{238}U in this energy range were resolved at a few scattering angles chosen to optimize the experimental resolution (usually 115 and/or 120 deg.). At these angles the intensity of the inelastic component was relatively large compared to the elastic contribution. Using flight paths in the range 8 to 11.8 meters the resolution of the 2+(45 keV) scattered-neutron group varied from very good at 1.5 MeV to marginal at 3.0 MeV as illustrated by the time-of-flight distributions of Fig. 9. Measurements were made at intervals of 0.3 MeV

from 1.5 to 3.0 and included ^{186}W and/or bismuth samples with the ^{238}U sample. The ^{186}W or bismuth measurements were used to determine the shape of the experimental resolution functions. These were well described by a least-squares fit of a Gaussian distribution as illustrated, for example, by the curves of Fig. 6. This resolution function was then least-squares fitted to the observed ^{238}U time distributions with the Gaussian width constrained to the value obtained from the bismuth or ^{186}W measurements. The relative intensities of the ^{238}U elastic and inelastic (2+, 45 keV) components were determined from the parameters obtained in these fitting procedures. Generally, the Gaussian fits were descriptive of the measured ^{238}U distributions as illustrated by the curves of Fig. 9. In addition, they were consistent with subjective estimates based upon graphical procedures.

The relative intensities of the elastic and inelastic neutron groups derived from the above fitting procedures were corrected for multiple scattering, beam attenuation, angular resolution and fission neutron contributions as outlined above. Following each good resolution, long-flight-path measurement, the detector was moved to a 5.5 flight path at an identical scattering angle and the collective response of the detector to ^{238}U elastic and inelastic (45 keV) scattered neutrons determined relative to the H(n,n) cross section. These shorter flight-path measurements were a part of the angular distribution measurements discussed above. Knowing the cross sections for the sum of the elastic and inelastic (45 keV) components and their relative intensities, the cross sections of the individual components follow directly. The resulting differential values are given in Table 3 together with the angle-integrated values deduced from the experimental results using the theoretical extrapolations of

Sec. V. The estimated uncertainties in the cross section values are based upon counting statistics, normalization and correction factors, and subjective judgements of the uncertainties due to the interpretation of the experimental resolutions. The latter considerations were a predominant factor at the higher energies (e.g., at 3.0 MeV).

The results of the above four Data Sets are reasonably consistent as illustrated by the composite of the values shown in Fig. 5. The largest discrepancies are associated with the lowest energy values of Data Set-3 which, as noted above, are of dubious quality. The agreement is despite the fact that the results were obtained using widely varying detectors, different experimental arrangements, varying sample sizes and configurations and spanned a period of nearly five years.

IV. COMPARISONS WITH PREVIOUS EXPERIMENTAL RESULTS

The 550 keV elastic scattering results of Data Set-2 are in good agreement with the previously reported values of Barnard et al. I(3) and of Smith (2) as illustrated in Fig. 10. The only region of minor discrepancy is at forward angles (e.g., 30 and 45 deg.) where the present results may be a few percent lower than those of Refs. 2 and 3. The results of Cranberg and Levin (1) are a composite of elastic and inelastic (2+, 45 keV) components. When corrected for the inelastic contribution, they agree very well with the present elastic scattering values. Small-angle (less than 20 deg.) elastic scattering results reported by Walt et al. (32) and Ankin et al. (33) are not entirely consistent but generally extrapolate to the elastic scattering results of the present work.

The present 550 keV differential cross sections for

the excitation of the 2+(45 keV) state are in good agreement with those reported by Barnard et al. I (3) as illustrated in Fig. 10. They are also reasonably consistent with the work of Cranberg and Levin (1) at scattering angles greater than 90 deg. but the single point of Ref. 1 forward of 90 degs. is somewhat below the present results. The results of Barnard et al. II (4) and of Smith (2) show the same angular-dependence as the present values but tend to be 5 to 10 percent smaller in magnitude. This difference is discussed below.

Generally, the relative angular dependence of scattered neutrons resulting in the excitation of the 45 keV state as obtained in the various measurements is similar and thus there is relatively little uncertainty in deriving the angle-integrated 550 keV cross section from a single or limited number of differential values.

The angle-integrated cross sections for the excitation of the 2+(45 keV) state derived from the present measurements are compared with those previously reported in Fig. 11. In making this (and similar) comparisons of angle-integrated quantities, previously reported differential values were converted to the angle-integrated cross sections in a manner identical to that employed in the interpretation of the present work. For example, 550 keV 90 deg. differential cross sections for the excitation of the 2+(45 keV) state were multiplied by four pi and then reduced by approximately 8 percent to account for the anisotropy observed experimentally and predicted by theory. The present results for the excitation of the 45 keV state were consistent with a broad energy average (e.g., a 100 keV energy average) of the results reported by Barnard et al. II (4). The fluctuations indicated in the work of Ref. 4 were not evident in the present results. Above incident neutron energies of approximately 550 keV

the present results for the excitation of the 45-keV state are consistent with those of Barnard et al. I (3) and of Cranberg and Levin (1). However, below approximately 400 keV the present results are much larger than those of Ref. 3. Above approximately 900 keV the present results are reasonably consistent with those of Egan et al. (7). The latter are somewhat larger but the differences may be associated with the choice of the angular distributions used in converting the isolated differential values to angle-integrated quantities. Moreover, the energy resolution of both experiments is probably no more than marginal in the higher energy range of 2.5 to 3.0 MeV. Above approximately 700 keV the present results agree with those reported by Smith (2). At lower energies the present results tend to be systematically higher than those of Ref. 2 by 5 to 10 percent though the values are within the respective uncertainties of the two data sets. The results of Ref. 2 were obtained at this laboratory more than a decade ago and even at this late date it is possible to estimate some sources of differences between these and the present results in the low energy region. With the possible exception of the 550-keV energy data, the resolution of the earlier work was not as good as that of the present results and at that energy the differences between the two sets of measurements is small (approximately 4.5 percent). The results of Ref. 2 are based upon a somewhat different carbon-reference cross section than the present work and that can account for a few percent of the difference. The earlier work was corrected for multiple scattering effects but not with the care given in the present measurements. As a consequence, it is estimated that several more percent of the difference can be attributed to multiple scattering effects, particularly at the

lower incident neutron energies. In the course of the present detailed studies of multiple scattering corrections, the importance of the corrections became very obvious. It is suspected that a number of the previously reported results were deficient in the applications of such corrections. There are marked differences between the present results and those of the evaluated data file ENDF/B-IV (19) at both low (less than 500 keV) and high (greater than 1.0 MeV) energies.

The angle-integrated cross sections for the excitation of the 4+(148 keV) state of the present work are consistent with those of Barnard et al. I (3), Cranberg and Levin (1), Barnard et al. II (4) and Smith (2), as illustrated in Fig. 11. In addition, the present results are in reasonable agreement with those of Egan et al. (7) et incident neutron energies in the range 0.9 to 2.1 MeV. Above 2.0 MeV the present values tend to be somewhat lower than those of Ref. 7. But the cross sections are small, and there are uncertainties in the interpretation of the few measured values in the context of unmeasured angular distributions. The present values are reasonably consistent with those of the evaluated data file ENDF/B-IV (19) to energies of approximately 15MeV. At higher energies its values in ENDF/B-IV are appreciably lower.

The present cross-sections for the excitation of the 6+(308 keV) state are compared with the single previously reported quantitative value of Cranberg and Levin (1) in Fig. 11. All of the cross sections for the excitation of this state are small and relatively uncertain. The measured values are reasonably consistent with those given in ENDF/B-IV.

V. PHYSICAL INTERPRETATION

The theoretical model essential to the determination of the angle-integrated inelastic scattering cross sections from the measured differential values was developed from a detailed study of the similar rotational nucleus, ^{186}W. As outlined above, it was possible to experimentally determine the differential elastic and inelastic (2+, 122 keV and 4+, 399 keV) scattering cross sections of ^{186}W over a wide angle-energy range. From this experimental base a coupled-channel model was developed for ^{186}W that provided an excellent description of the observed cross sections as illustrated in Fig. 7. This model and its physical implications are discussed in detail in Ref. 30. The essential relevance to the present ^{238}U work is the capability of the model to extrapolate a single or few differential inelastic cross sections for the excitation of the ground-state rotational band to angle-integrated values. The ^{186}W study shows that the cross sections for the excitation of the ground-state rotational band at few MeV energies can be largely attributed to direct reactions and that the associated scattered neutron distributions are not only highly anisotropic but also strongly forward peaked.

The above model was applied to ^{238}U assuming an N, Z and A dependence of the real potential of the form $-24\ (N-Z)/A$ (MeV) (34). The beta-2 and beta-4 deformations were taken from Moller (35) and LaGrange (36). The ^{186}W-based potential was slightly adjusted (primarily a small reduction in real-potential strength) to improve the description of the observed composite ^{238}U elastic and inelastic (2+, 45 keV) distribution in the range 2.5 to 3.0 MeV. It was assumed that compound-nucleus contributions to the distributions at these

energies were essentially negligible. The initial calculations were made coupling the ground- and first-excited-state using the computer program 2 PLUS (37). Subsequently, the calculations were refined to include the 4+(148 keV) channel and the beta-4 deformation using the computer program JUPITER (38). The calculations were then extended to lower energies and the compound-nucleus processes. The latter were calculated from the Hauser-Feshbach formula with width-fluctuation corrections using the computer program NEARREX (39). At incident energies of less than 1.0 MeV, the excited structure of ^{238}U is reasonably known and the compound-nucleus channels can be explicitly calculated (28). At excitation energies above approximately 1.0 MeV the structure becomes increasingly uncertain and the calculated compound-nucleus contributions had to be corrected for competition from unknown channels using statistical estimates. At incident energies below approximately 1.0 MeV, radiative capture processes were a contributing factor. These were calculated using the computer program CASCADE (40). An additional factor at lower energies was the correlation effect discussed by Moldauer (41). It was estimated using NEARREX. The suitability of the model for calculating higher-energy composite elastic and inelastic (45 keV) scattering cross sections of ^{238}U is illustrated in Fig. 8. Detailed comparisons of measured and calculated 550 keV scattering cross sections are given in Fig. 10. At this low energy the correlation parameter, Q (41), was adjusted to obtain inelastic (45 keV) cross section magnitudes relatively consistent with experimental observation. Generally, Q had a value near unity; indicating significant correlation enhancement of the inelastic channel. The calculated inelastic distributions at 550 keV were not as forward peaked as indicated by the present

experiments and those of Ref. 2. The difference is probably physically significant but the angle-integrated cross sections derived from the differential values using either the calculated relative distributions or those obtained from a least-square fit to the measured values differed by only several percent. The neutron total cross sections calculated with the model for energies in the range 0.2 to 3.0 MeV differed by less than 5 percent from measured values reported in the literature (10). The ability of the model to describe this wide range of experimental results gives confidence in its use for extrapolating measured differential results to obtain angle-integrated cross sections. The model parameters and form factors are given in Table 4. They are similar to those of LaGrange (36) with a somewhat smaller real-potential strength.

The deduction of the angle-integrated values from the differential cross sections involved only a relative extrapolation. The normalization remained experimental. The resulting angle-integrated cross sections are given in Tables 1, 2 and 3 and illustrated in Figs. 5 and 11. The uncertainties in the extrapolation procedures were difficult to estimate quantitatively, particularly in the few MeV range. However, wide variations in the model did not appreciably change the extrapolated results. For example, at an incident energy of 2.7 MeV: 1) the angle-integrated cross section for the excitation of the 45 keV state obtained using the potentials of Dunford et al. (37) and of LaGrange (36) differed from those obtained with the above potential by less than 10 percent, 2) changes in beta-2 of ± 25 percent lead to less than 5 percent changes in the angle-integrated value, and 3) results obtained with the 2-PLUS program, neglecting the excitation of the 148 keV state and the beta-4 deformation, were

within 10 percent of the more comprehensive results obtained with JUPITOR. These variations were generally not of the same sign. At lower energies (e.g., 550 keV) there was little difference between angle-integrated cross sections obtained using the model for extrapolation and angular distributions determined from least-square fits to the experimental data. Tests such as the above do not insure against a systematic error but they do give some confidence in the model-extrapolated results.

Cross sections predicted by the model (including normalization) were in reasonable agreement with the experimentally normalized values as illustrated in Fig. 11. The calculations for the excitation of the 45 keV state at lower energies (e.g., less than 600 keV) were not unambiguous. These cross sections are largely due to compound-nucleus processes governed by transmission coefficients which are influenced by deformation, fluctuations and correlations in an uncertain manner. The illustrated calculational results were obtained with a deformed potential (37) and corrected for fluctuations, correlations and radiative capture. Alternate derivations were examined including: a) simple spherical potentials and the Hauser-Feshbach formula, b) only corrections for fluctuation effects, c) various choices of the correlation parameter Q, and d) differing strengths for the channel-coupling. The various calculational results, when normalized to the well established experimental value of 1.6 b at 550 keV, deviated from the results illustrated in Fig. 11 by as much as ±15 percent at 300 keV. These differences represent considerable variation in the energy-dependent shape of the cross section near threshold as calculated with the various models. However, all of the calculated results when normalized to the 550 keV measured value were inconsistent with the low-energy cross sections of the 45 keV state as given in ENDF/B-IV and as reported in

some previous experimental measurements. Theoretical uncertainties at lower energies may be further reflected in the calculated excitations of the 148 keV state which are consistently smaller than the body of the experimental information to energies of 1.0 MeV. In the few MeV range the calculated cross sections for the excitation of the 45 and 148 keV states are in reasonable agreement with the experimental values. The calculations indicate that the direct-reaction mechanism is a major factor in this higher-energy region. Calculated and measured cross sections for the excitation of the 308 keV state are relatively consistent at energies above $\tilde{\sim}$ 1.0 MeV. Below 1.0 MeV the calculations indicate smaller cross sections for the excitation of the 308 keV than observed experimentally. However, the comparisons are not particularly meaningful due to the relatively large experimental uncertainties.

VI. EVALUATED DATA SETS

The evaluated data sets for the excitation of the 45, 148 and 308 keV states were constructed from the above measured values and associated calculations, and from experimental values selected from the literature.

The evaluated cross sections for the excitation of the 45 keV state were normalized to the measured values at the experimentally favorable energy of 550 keV. At this energy the results of the present work, those of Barnard et al. I(3) and of Cranberg and Levin (1) are in very good agreement. The results of Smith (2) are slightly lower and a broad energy average of the results of Barnard et al. II (4), slightly higher. The 550 keV scattered-neutron angular distributions are known reasonably well and from them it is possible to determine the angle-integrated cross section values. Below 550 keV this evaluation follows the present results and is consistent with the broad energy average of those of Barnard et al. II (4). The structure indicated in

the latter results was not accepted, as it could not be verified in the present experiments. The other major data set in the low energy region, that of Ref. 3, is much lower than the present results and has a different energy-dependent behavior. It was not used in the low energy portions of the present evaluation. Two low-energy values were obtained at this laboratory a number of years ago (2). However, they are relatively uncertain and suspect, as discussed above, and thus they were not considered in the evaluation. The evaluation in the range 500 to 1200 keV follows the available experimental information relatively interpolated with theory. The data base in this region is large and relatively consistent (1,2,3,4,5, and 6). From 1.2 to 3.0 MeV, the evaluation relies primarily upon the present work and that of Egan et al. (7). The two sets of measurements and the theoretical calculations are in reasonable agreement and the evaluation is a compromise between the various measured and the calculated values. Above 3.0 MeV, the evaluation is based entirely upon the above calculational model. The estimated uncertainties in the evaluated cross sections for the excitation of the 45-keV state are: a) less than 5 percent at 550 keV, b) less than 15 percent below 550 keV, c) less than 10 percent from 550 to 1500 keV and d) less than 25 percent from 1.5 to 3.0 MeV.

The experimental cross sections for the excitation of the 148-keV state are reasonably consistent to approximately 1.5 MeV (1,2,3,4,6 and 7). The evaluation was subjectively deduced from these measured values. The uncertainty is estimated to be approximately 10 percent. Both the evaluation and the experimental results are somewhat larger than the theoretically predicted cross sections near threshold as discussed above. From

1.5 to 3.0 MeV MeV the evaluation is based upon the present work and the results of Egan et al. (7). In this region the uncertainties are estimated to be less than 25 percent. Above 3.0 MeV the evaluation is derived entirely from the above calculational model.

The experimental cross sections for the excitation of the 308-keV state are confined to the present work and a single result of Ref. 1. All of the measured values are small and relatively uncertain. Further, they tend to be systematically larger than those estimated by theory. The experiments are very difficult and may have tended toward too large cross section values. The evaluation compromises between measured and calculated quantities. The uncertainties may be as much as 50 percent but are probably of little concern in most applications due to the very small magnitudes of the cross sections.

The angular distributions associated with the above evaluated inelastic scattering cross sections were determined from the experimental values where possible (e.g., at 550 keV). However, over much of the energy range primary reliance had to be placed upon relative angular distributions derived from the above model. In addition the cross sections for the excitation of the 308-keV were simply assumed to be isotropic at all energies.

The numerical values of the above evaluated data sets are given in Appendix, and the results are compared with the measured values and the corresponding portions of ENDF/B-IV in Fig. 12. Below approximately 500 keV the present evaluation differs appreciably from ENDF/B-IV in both magnitude and energy-dependent shape. At some energies the present evaluation is as much as 30 percent larger than that of ENDF/B-IV. There is also an appreciable difference between the present evaluation and

that of ENDF/B-IV above approximately 1.0 MeV with the present results much the larger. The angular distributions associated with the excitation of the 45- and 148-keV states are given as isotropic in ENDF/B-IV and, at higher energies, are much different than those of the present evaluation.

The use of the present evaluation in neutronic calculations (e.g., fast reactor calculations) may lead to considerably different results than obtained with ENDF/B-IV. The major influence will probably be at low energies. At energies above approximately 1.0 MeV the present inelastic scattering cross sections show large contributions due to the excitation of the first two states. These are largely achieved at the expense of the elastic scattering cross sections. Many applications may not be particularly sensitive to the relatively small differences in the associated energy transfer. However, a complete re-interpretation of inelastic neutron scattering from ^{238}U in the few MeV range in light of the recent measurements may lead to reduced inelastic scattering cross sections for large energy transfer. Such a comprehensive examination is now in progress.

VII. SUMMARY REMARK

The measurements give improved definition to the cross sections for the neutron excitation of the ground-state rotational band of ^{238}U (2+, 45 keV, 4+, 148 keV and 6+, 308 keV) at selected scattering angles from near threshold to 3.0 MeV. Differential cross sections for the elastic and the inelastic (45 keV) scattering of 550 keV neutrons were measured to few percent accuracies over the angular range 30 to 150 deg. The composite differential cross sections for elastic and inelastic (45 keV) scattering were measured from 1.5 to 3.0 MeV over the angular

range 20 to 150 deg. A coupled-channel and statistical nuclear model, developed in the context of the similar nucleus ^{186}W, was descriptive of the measured ^{238}U cross sections and was used to extrapolate the differential results to angle-integrated values. The present results indicate a cross section for the excitation of the 45-keV state considerably larger than those reported from some previous measurements or as given by ENDF/B-IV at energies of less than approximately 500 keV. Above approximately 1.0 MeV the present cross sections for the excitation of the 45 and 148 keV states are again appreciably larger than those given by ENDF/B-IV. The model indicates that the ^{238}U inelastic scattering cross sections at energies of less than 1.0 MeV are dominated by the compound-nucleus process though there remain uncertainties as to the quantitative nature of the reaction mechanism. In the few-MeV range the model indicates that these inelastic cross sections are very largely due to direct-reaction mechanisms. The results of the present work and selected values from the literature are used to construct an evaluated data set suitable for applied use.

REFERENCES

1. L. Cranberg and J. Levin, Phys. Rev., 109 (1958) 2063, See also Los Alamos Scientific Lab. Report LA-2177.
2. A. Smith, Nucl. Phys., 47 (1963) 633.
3. E. Barnard, A. Ferguson, W. McMurray and I. Van Heerdon, Nucl. Phys., 80 (1966) 46.
4. E. Barnard, J. De Villiers and D. Reitmann, 2nd Inter. Conf. on Nucl. Data for Reactors, VOL-2, P-103, IAEA Press, Vienna (1970).
5. L. Stromberg and S. Schwartz, Nucl. Phys., 71 (1965) 511.
6. P. Guenther and A. Smith, 4th Conf. on Nuclear Cross Sections and Technology, Washington (1975) Paper IB-3, Preliminary portions of the present work were reported here.
7. J. Egan, G. Kegek, G. Couchell, A. Mittler, B. Barnes, W. Schier, D. Fullen, P. Harihar, T. Marcella, N. Sullivan, E. Sheldon and A. Prince, 4th Inter. Conf. on Nuclear Cross Sections and Technology, Washington (1974) Paper IB-26.
8. J. Lynn, Atomic Energy Research Establishment Report, AERE-R-7468, (1974).
9. P. Lambropolous, Nucl. Sci. and Eng., 46 (1971) 356.
10. A. Smith, Argonne National Lab. Memorandums, (1973 and 1974) Unpublished.
11. J. Beery, K. Harper, V. Stovall and L. Rosen, Los Alamos Sci. Lab. Report, LASL-3788 (1968).
12. D. Chase and L. Willets, Bull. Am. Phys. Soc., 2 (1957) 72.
13. L. Dresner, Nucl. Sci. and Eng., 1 (1956) 501.
14. S. Yiftah, D. Okrent and P. Moldauer, Fast Reactor Cross Sections, Pergamon Press, New York (1960).
15. CH. LaGrange, NEANDC Report, JAERI-M-5984 (1975).
16. G. Palla, Phys. Let., 358 (1971) 477.
17. C. Dunford, Proc. of Conf. on Nucl. Data for Reactors, Paris, 1 (1967) 429, IAEA Press, Vienna.
18. W. McMurray, Southern Univ. Ann. Research Report, (1973).
19. Evaluated Nuclear Data File-B, ENDF/B, Available from the National Neutron Cross Section Center, Brookhaven National Laboratory, Herein we refer to Version IV of ENDF/B.
20. H. Newson and J. Gibbons, Fast Neutron Physics, Part-2, p-1601, Ed. by J. Marion and J. Fowler, Interscience Pub., New York (1963).

21. S. Cox and P. Hanley, Bull. Am. Phys. Soc., 60 (1971) 221.
22. A. Smith, P. Guenther, R. Larsen, C. Nelson, P. Walker and J. Whalen, Nucl. Instr. and Methods 50 (1967) 277.
23. P. Guenther, A. Smith and J. Whalen, ZR-90 and Zr-92 Neutron Total and Scattering Cross Sections, submitted to the Phys. Rev.
24. G. Duffy, S. Buccino and A. Smith, Argonne National Lab. Report a Computer Program for Processing Fast Neutron Scattering Data, Unpublished (1966).
25. A. Smith and P. Guenther, Argonne National Lab. Memorandum, Program for the Acquisition and Reduction of Data, Unpublished (1975).
26. A. Langsdorf, R. Lane and J. Monahan, Argonne National Lab. Report ANL-5567 (Rev), (1961).
27. J. Hopkins and G. Breit, Nuclear Data A9 (1971) 137.
28. Nuclear Data Sheets for A=238, Y. Ellis (1970).
29. A. Hanson and J. McKibben, Phys. Rev., 72 (1947) 673.
30. P. Guenther, A. Smith and J. Whalen, Fast Neutron Interactions with Tungsten 186, to be published.
31. R. Holt and A. Smith, 4th Conf. on Nuclear Cross Sections and Technology, Washington (1975), Paper DB-5.
32. M. Walt and D. Fossan, Phys. Rev., 137B (1965) 629.
33. G. Anikin and I. Kotukhov, YF 12 (6) (1971) 1121.
34. S. Tanaka, NEANDC Report JAERI-M-5984 (1975).
35. P. Moller, Nucl. Phys., A192 (1972) 529.
36. CH. LaGrange, National Soviet Conf. on Neut. Physics, Kiev (1975).
37. C. Dunford, Atomics International Report NAA-SR-11706 (1966).
38. T. Tamura, Oak Ridge National Lab. Report, ORNL-4132 (1967).
39. P. Moldauer, C. Engelbrecht and G. Duffey, Argonne National Lab. Report ANL-6978 (1964).
40. W. Poenitz, Private Communication (1975).
41. P. Moldauer, Phys. Rev., C11 (1975) 426.
42. W. P. Poenitz, Private Communication (1975).
43. D. Lister, A. Smith and C. Dunford, Phys. Rev., 162 (1967) 1077.
44. H. Knitter, M. Coppola, N. Ahmed and B. Jay, Ziets. Phys., 244 (1971) 358.
45. R. Batchelor, W. Gilboy and J. Towle, Nucl. Phys., 65 (1965) 236.

TABLE 1

Low Energy 90 deg. Differential Cross Sections for the Excitation of the 2+(45 keV) State of ^{238}U

Data Set-1

Energy(keV)[a]	Ratio $d\sigma(U)/d\sigma(C)$ at 90 deg.	$d\sigma(U)$, b/sr[b]	$\sigma(U)$, b[b,c]
611	0.575 ± 4.5%	0.137 ± 4.5%	1.58 ± 0.07
565	0.504 ± 5.0%	0.124 ± 5.0%	1.43 ± 0.07
535	0.528 ± 6.0%	0.132 ± 6.0%	1.53 ± 0.09
500	0.545 ± 5.0%	0.140 ± 5.0%	1.62 ± 0.08
475	0.472 ± 8.0%	0.126 ± 8.0%	1.45 ± 0.12
450	0.500 ± 8.0%	0.136 ± 8.0%	1.57 ± 0.12
425	0.463 ± 7.0%	0.128 ± 7.0%	1.48 ± 0.10
400	0.489 ± 7.0%	0.136 ± 7.0%	1.58 ± 0.11
375	0.508 ± 8.0%	0.144 ± 8.0%	1.66 ± 0.13
350	0.495 ± 7.0%	0.141 ± 7.0%	1.63 ± 0.11
325	0.468 ± 6.0%	0.138 ± 6.0%	1.59 ± 0.09
300	0.523 ± 12.0%	0.157 ± 12.0%	1.81 ± 0.22
275	0.469 ± 6.0%	0.143 ± 6.0%	1.65 ± 0.10
250	0.446 ± 12.0%	0.139 ± 12.0%	1.61 ± 0.19
225	0.391 ± 10.0%	0.124 ± 10.0%	1.43 ± 0.14
200	0.305 ± 14.0%	0.099 ± 14.0%	1.14 ± 0.16
175	0.349 ± 12.0%	0.115 ± 12.0%	1.33 ± 0.16
150	0.334 ± 20.0%	0.114 ± 20.0%	1.32 ± 0.26

Data Set-2

Energy(keV)[a]	Ratio $d\sigma(U)/d\sigma(C)$ at 90 deg.	$d\sigma(U)$, b/sr[b]
550	0.562 ± 7.0%	0.143 ± 7.0%
550	0.499 ± 7.0%	0.127 ± 7.0%
550	0.618 ± 8.0%	0.157 ± 8.0%
550	0.515 ± 9.0%	0.131 ± 9.0%
550	0.547 ± 9.0%	0.139 ± 9.0%
		Ave = 0.139 ± 4.0%
		$\sigma(U)$, b[c] = 1.606 ± 0.064

a. Incident energy, energy spread 10-15 keV.
b. Not inclusive of uncertainty in standard-reference value.
c. Corrected for anisotropy as defined in text, not inclusive of the estimated < 3% uncertainty in this correction.

TABLE 2

Inelastic Neutron Scattering Cross Sections of ^{238}U from Data Set-3

E_x(MeV)	E_{in}(MeV)	σ(b)	δσ(b)
0.045	0.400	1.20	0.21
	0.450	1.52	0.22
	0.500	1.32	0.23
	0.550	1.70	0.18
	0.563	1.50	0.15
	0.669	1.56	0.15
	0.731	1.40	0.14
	0.766	1.29	0.13
	0.853	1.02	0.12
	0.955	1.23	0.15
	1.100	0.95	0.14
	1.200	0.61	0.12
0.148	0.563	0.311	0.04
	0.669	0.416	0.04
	0.731	0.434	0.04
	0.766	0.425	0.04
	0.853	0.488	0.05
	0.955	0.533	0.08
	1.065	0.455	0.05
	1.122	0.533	0.05
	1.177	0.478	0.05
	1.222	0.414	0.06
	1.320	0.278	0.08
	1.397	0.321	0.05
	1.500	0.230	0.05
0.308	0.840	0.025	0.012
	0.955	0.037	0.018
	1.100	0.070	0.030
	1.150	0.069	0.030
	1.200	0.072	0.050
	1.400	0.038	0.020

TABLE 3

^{238}U Inelastic Scattering Results of Data Set-4

E_x (MeV)	E_{in} (MeV)	Angle (deg.)	$\frac{d\sigma}{d\Omega}$ (b/sr)	$\Delta \frac{d\sigma}{d\Omega}$ (%)	σ^a (b)
0.045	1.5	120	0.049	15	0.620±0.093
"	1.8	115	0.054	15	0.706±0.105
"	2.1	120	0.033	15	0.428±0.064
"	2.4	115	0.022	20	0.317±0.063
"	2.7	120	0.024	20	0.350±0.070
"	3.0	120	0.025	28	0.390±0.115
0.148	1.5	120	0.025	15	0.359±0.053
"	1.8	115	0.016	17	0.237±0.040
"	1.8	115	0.021	16	0.310±0.049
"	2.1	120	0.019	20	0.311±0.062
"	2.4	115	0.008	15	0.131±0.020
"	2.7	120	0.006	17	0.120±0.020
"	3.0	120	0.008	18	0.170±0.031
0.308	1.8	115	0.006	40	0.075±0.030

a. Angle integrated values deduced as discussed in Sec. III and V of text. Uncertainties are not inclusive of extrapolation to angle-integrated values.

TABLE 4

Model Parameters and Form Factors

Real Well, Saxon Form

V_r = 45.5, MeV

R = 1.24 · $A^{1/3}$, F

a = 0.62, F

Imaginary Well, Derivative Form

W_1 = 3.9, MeV

R = 1.26 · $A^{1/3}$, F

a = 0.58, F

Spin-orbit Well, Thomas Form

V_{so} = 7.5, MeV

Coupling Strength = V

Deformation

β_2 = 0.216, β_4 = 0.064

FIGURE CAPTIONS

Fig. 1. Representative neutron time-of-flight spectrum obtained in the measurements of Data Set-1. The elastic and inelastic (45 keV) neutron groups are reasonably well resolved.
(ANL Neg. No. 116-75-69)

Fig. 2. Low-energy cross sections for the neutron excitation of the 45-keV state of ^{238}U. The circular data points are from Data Set-1 and the solid square point from Data Set-2. The solid curve indicates the present evaluation, the dashed curve that of ENDF/B-IV and the dotted curve the results of theoretical calculation.
(ANL Neg. No. 116-75-71)

Fig. 3. Representative neutron time-of-flight spectra obtained in the measurements of Data Set-2. The 30 deg. distribution is the "worst case" with a large difference between the relative magnitude of elastic and inelastic (45 keV) components. The 90-deg. distribution is typical of those obtained at scattering angles greater than approximately 60 deg.
(ANL Neg. No. 116-75-72)

Fig. 4. Measured differential elastic (○) and inelastic (□, 45-keV state) neutron scattering cross sections of ^{238}U. The curves indicate the results of a least-squares fit of a Legendre polynomial series to the measured values.
(ANL Neg. No. 116-75-65)

Fig. 5. Measured cross sections for the excitation of the 45-keV and of the 148-keV states as obtained in Data Set-1 (○), Data Set-2 (□), Data Set-3 (△) and Data Set-4 (⋈). The solid curve indicates the present evaluation and the dashed curve that of ENDF/B-IV. The dotted curve indicates the results of theoretical calculation as discussed in Sec. V of the text.
(ANL Neg. No. 116-75-70)

Fig. 6. Neutron time-of-flight spectrum observed by scattering 1.8 MeV neutrons from ^{186}W. The histogram indicates experimental values and the curves, the result of a two-Gaussian least-squares fit to the measured values. The two peaks correspond to elastic and inelastic (excitation of the 122 keV state) scattered neutrons.
(ANL Neg. No. 116-2475)

Fig. 7. Differential elastic and inelastic (E_x = 122 keV) scattering cross sections of ^{186}W. Data points indicate measured values

and curves the results of model calculations.
(ANL Neg. No. 116-75-125)

Fig. 8. Measured composite differential cross sections for elastic and inelastic scattering (45 keV) from ^{238}U at 1.5, 1.8, 2.1, 2.7 and 3.0 MeV incident neutron energies. The present experimental results are noted by O. Previously-reported measurements are: ◁ Ref. 44, X Ref. 1 and + Ref. 45. Some of the illustrated previous values differ by as much as 10 percent in incident energy from the present results (e.g., Ref. 44 is at 1.9 MeV), and in these instances there are differences between measured values. The curves indicate the results of theoretical calculation as discussed in Sec. V of the text.
(ANL Neg. No. 116-75-67)

Fig. 9. Illustrative neutron time-of-flight spectra obtained by scattering 1.5, 1.8 and 2.7 MeV neutrons from ^{238}U. Histograms represent the experimental values and curves the results of Gaussian fitting procedures as described in Sec. III of the text. The elastic and inelastic (45 and 148 keV) neutron groups are evident. Scattering angles were in the range 115 to 120 deg. and flight paths varied from 8 to 11.8 meters.
(ANL Neg. No. 116- 75-73)

Fig.10. Comparison of measured differential elastic and inelastic (45 keV) scattering cross sections of ^{238}U at 550 keV. The present measured values are represented by circular data points: those of Ref. 3 by △, Ref. 1 by +, Ref. 2 by ⋋, Ref. 4 by ⋈, Ref. 32 by and Ref. 33 by . The elastic scattering values of Ref. 1 include the 45 keV inelastic-scattering component. The curves indicate the results of theoretical calculation as discussed in Sec. V of the text.
(ANL Neg. No. 116-75-66)

Fig.11. Comparisons of measured, calculated and evaluated cross sections for the neutron excitation of the 45, 148 and 308 keV states of ^{238}U. The present measured values are indicated by square data points: those of Ref. 2 by O, Ref. 3 △, Ref. 4 , Ref. 1 X, and Ref. 7 +. The solid curve indicates the present evaluation, the dashed curve that of ENDF/B-IV and the dotted curve the results of the theoretical calculations discussed in Sec. V of the text.
(ANL Neg. No. 116-75-68)

Appendix; Numerical Evaluated Data Set.

```
 9.22380+ 4 2.36006+ 2                  0          01          0          238 3  0 2198
 0.0    + 0-.45     +05                 0           0          1        0 238 3 51 2199
         26          2                                                  26 238 3 51 2200
 .45189E 05 .00000E 00 .75000E 05 .49000E 00 .10000E 06 .84000E 00                238 3 51 2201
 .15000E 06 .12000E 01 .20000E 06 .13800E 01 .25000E 06 .14900E 01 238 3 51 2202
 .30000E 06 .15600E 01 .35000E 06 .15800E 01 .40000E 06 .16000E 01 238 3 51 2203
 .50000E 06 .15850E 01 .60000E 06 .15650E 01 .70000E 06 .14600E 01 238 3 51 2204
 .80000E 06 .13000E 01 .10000E 07 .10300E 01 .12000E 07 .84300E 00 238 3 51 2205
 .15000E 07 .69300E 00 .18000E 07 .57800E 00 .21000E 07 .50000E 00 238 3 51 2206
 .27000E 07 .43500E 00 .30000E 07 .43000E 00 .40000E 07 .40000E 00 238 3 51 2207
 .60000E 07 .33570E 00 .80000E 07 .28900E 00 .10000E 08 .24600E 00 238 3 51 2208
 .14000E 08 .22000E 00 .20000E 08 .20000E 00 .00000E 00 .00000E 00 238 3 51 2209

 9.22380+ 4 2.36006+ 2                  0          02          0          238 3  0 2211
 0.0    + 0-.148    +06                 0           0          1        0 238 3 52 2212
         15          2                                                  15 238 3 52 2213
 .14862E 06 .00000E 00 .40000E 06 .15000E 00 .60000E 06 .30000E 00                238 3 52 2214
 .80000E 06 .43000E 00 .10000E 07 .50000E 00 .12000E 07 .44500E 00 238 3 52 2215
 .15000E 07 .37800E 00 .18000E 07 .30500E 00 .21000E 07 .24000E 00 238 3 52 2216
 .24000E 07 .19220E 00 .27000E 07 .15400E 00 .30000E 07 .14900E 00 238 3 52 2217
 .60000E 07 .10500E 00 .10000E 08 .60000E-01 .20000E 08 .38000E-01 238 3 52 2219

 9.22380+ 4 2.36006+ 2                  0          03          0          238 3  0 2220
 0.0    + 0-.308    +06                 0           0          1        0 238 3 53 2221
         9           2                                                   9 238 3 53 2222
 9.22380+ 4 2.36006+ 2                  0          2           0          238 3 53 2223
 0.0    + 0 2.36006+ 2                  0          2           0        0 238 4 51 2770
 0.0    + 0 0.0    + 0                  0          2           0        0 238 4 51 2771
         9           2                  0          0           1        9 238 4 51 2772
 0.0    + 0 .45189 + 5                  0          0           0        0 238 4 51 2773
         2           2                  0          0           1        2 238 4 51 2774
-1.0    + 0 0.5    + 0 1.0    + 0 0.5  + 0 0.0    + 0 0.0    + 0        0 238 4 51 2775
 0.0    + 0 0.5    + 6                 0          0           1       31 238 4 51 2777
         31          2                  0          0           0        0 238 4 51 2778
-.10000E 01 .35380E 00-.99452E 00 .35519E 00-.97815E 00 .35931E 00 238 4 51 2779
-.95106E 00 .36602E 00-.91354E 00 .37513E 00-.86602E 00 .38634E 00 238 4 51 2780
-.80902E 00 .39931E 00-.74314E 00 .41364E 00-.66913E 00 .42892E 00 238 4 51 2781
-.58778E 00 .44468E 00-.50000E 00 .46049E 00-.40674E 00 .47593E 00 238 4 51 2782
-.30902E 00 .49061E 00-.20791E 00 .50417E 00-.10453E 00 .51633E 00 238 4 51 2783
 .13269E-05 .52687E 00 .10453E 00 .53566E 00 .20791E 00 .54261E 00 238 4 51 2784
 .30902E 00 .54774E 00 .40674E 00 .55114E 00 .50000E 00 .55294E 00 238 4 51 2785
 .58779E 00 .55336E 00 .66913E 00 .55264E 00 .74315E 00 .55105E 00 238 4 51 2786
 .80902E 00 .54890E 00 .86603E 00 .54647E 00 .91355E 00 .54405E 00 238 4 51 2787
 .95106E 00 .54187E 00 .97815E 00 .54016E 00 .99452E 00 .53907E 00 238 4 51 2788
 .10000E 01 .53870E 00 .00000E 00 .00000E 00 .00000E 00 .00000E 00 238 4 51 2789
 0.0    + 0 0.1    + 7                 0          0           1       31 238 4 51 2790
         31          2                  0          0           0        0 238 4 51 2791
-.10000E 01 .35380E 00-.99452E 00 .35519E 00-.97815E 00 .35931E 00 238 4 51 2792
-.95106E 00 .36602E 00-.91354E 00 .37513E 00-.86602E 00 .38634E 00 238 4 51 2793
-.80902E 00 .39931E 00-.74314E 00 .41364E 00-.66913E 00 .42892E 00 238 4 51 2794
-.58778E 00 .44468E 00-.50000E 00 .46049E 00-.40674E 00 .47593E 00 238 4 51 2795
 .13269E-05 .52687E 00 .10453E 00 .53566E 00 .20791E 00 .54261E 00 238 4 51 2796
 .30902E 00 .54774E 00 .40674E 00 .55114E 00 .50000E 00 .55294E 00 238 4 51 2797
 .58779E 00 .55336E 00 .66913E 00 .55264E 00 .74315E 00 .55105E 00 238 4 51 2798
 .80902E 00 .54890E 00 .86603E 00 .54647E 00 .91355E 00 .54405E 00 238 4 51 2799
 .95106E 00 .54187E 00 .97815E 00 .54016E 00 .99452E 00 .53907E 00 238 4 51 2800
 .10000E 01 .53870E 00 .00000E 00 .00000E 00 .00000E 00 .00000E 00 238 4 51 2801
```

```
 0,0     + 0 0,15    + 7            0              0              1            31 238 4 51 2803
           31            2            0              0              0             0 238 4 51 2804
-,100000E 01 ,43580E 00-,99452E 00 ,43757E 00-,97815E 00 ,44272E 00 238 4 51 2805
-,951106E 00 ,42084E 00-,91354E 00 ,46111E 00-,86602E 00 ,47235E 00 238 4 51 2806
-,809026E 00 ,48308E 00-,74314E 00 ,49174E 00-,66913E 00 ,49704E 00 238 4 51 2807
-,587786E 00 ,49834E 00-,50000E 00 ,49590E 00-,40674E 00 ,49094E 00 238 4 51 2808
-,309026E 00 ,48542E 00-,20791E 00 ,48152E 00-,10453E 00 ,48111E 00 238 4 51 2809
 ,132696E-05 ,48514E 00 ,10453E 00 ,49337E 00 ,20791E 00 ,50440E 00 238 4 51 2810
 ,309026E 00 ,51606E 00 ,40674E 00 ,52598E 00 ,50000E 00 ,53232E 00 238 4 51 2811
 ,587796E 00 ,53418E 00 ,66913E 00 ,53163E 00 ,74315E 00 ,52651E 00 238 4 51 2812
 ,809026E 00 ,51997E 00 ,86603E 00 ,51368E 00 ,91355E 00 ,50939E 00 238 4 51 2813
 ,951106E 00 ,50685E 00 ,97815E 00 ,50569E 00 ,99452E 00 ,50579E 00 238 4 51 2814
 ,100000E 01 ,50585E 00 ,00000E 00 ,00000E 00 ,00000E 00 ,00000E 00 238 4 51 2815
 0,0     + 0 0,21    + 7            0              0              1            31 238 4 51 2816
           31            2            0              0              0             0 238 4 51 2817
-,100000E 01 ,39389E 00-,99452E 00 ,39736E 00-,97815E 00 ,40752E 00 238 4 51 2818
-,951106E 00 ,42355E 00-,91354E 00 ,44377E 00-,86602E 00 ,46549E 00 238 4 51 2819
-,809026E 00 ,48511E 00-,74314E 00 ,49881E 00-,66913E 00 ,50347E 00 238 4 51 2820
-,587786E 00 ,49785E 00-,50000E 00 ,48330E 00-,40674E 00 ,46386E 00 238 4 51 2821
-,309026E 00 ,44549E 00-,20791E 00 ,43450E 00-,10453E 00 ,43572E 00 238 4 51 2822
 ,132696E-05 ,45096E 00 ,10453E 00 ,47619E 00 ,20791E 00 ,51199E 00 238 4 51 2823
 ,309026E 00 ,54504E 00 ,40674E 00 ,57019E 00 ,50000E 00 ,58264E 00 238 4 51 2824
 ,587796E 00 ,58124E 00 ,66913E 00 ,56875E 00 ,74315E 00 ,55075E 00 238 4 51 2825
 ,809026E 00 ,53374E 00 ,86603E 00 ,52296E 00 ,91355E 00 ,52086E 00 238 4 51 2826
 ,951106E 00 ,52635E 00 ,97815E 00 ,53567E 00 ,99452E 00 ,54397E 00 238 4 51 2827
 ,100000E 01 ,54725E 00 ,00000E 00 ,00000E 00 ,00000E 00 ,00000E 00 238 4 51 2828
 0,0     + 0 0,30    + 7            0              0              1            31 238 4 51 2829
           31            2            0              0              0             0 238 4 51 2830
-,100000E 01 ,22462E 00-,99452E 00 ,22354E 00-,97815E 00 ,22782E 00 238 4 51 2831
-,951106E 00 ,25408E 00-,91354E 00 ,31417E 00-,86602E 00 ,40264E 00 238 4 51 2832
-,809026E 00 ,49416E 00-,74314E 00 ,55386E 00-,66913E 00 ,55537E 00 238 4 51 2833
-,587786E 00 ,49652E 00-,50000E 00 ,40226E 00-,40674E 00 ,31607E 00 238 4 51 2834
-,309026E 00 ,27624E 00-,20791E 00 ,30824E 00-,10453E 00 ,39652E 00 238 4 51 2835
 ,132696E-05 ,51056E 00 ,10453E 00 ,61107E 00 ,20791E 00 ,66936E 00 238 4 51 2836
 ,309026E 00 ,67754E 00 ,40674E 00 ,64766E 00 ,50000E 00 ,60232E 00 238 4 51 2837
 ,587796E 00 ,56268E 00 ,66913E 00 ,54154E 00 ,74315E 00 ,53981E 00 238 4 51 2838
 ,809026E 00 ,55237E 00 ,86603E 00 ,57216E 00 ,91355E 00 ,59391E 00 238 4 51 2839
 ,951106E 00 ,61442E 00 ,97815E 00 ,63156E 00 ,99452E 00 ,64318E 00 238 4 51 2840
 ,100000E 01 ,64732E 00 ,00000E 00 ,00000E 00 ,00000E 00 ,00000E 00 238 4 51 2841
 0,0     + 0 0,60    + 7            0              0              1            31 238 4 51 2842
           31            2            0              0              0             0 238 4 51 2843
-,100000E 01 ,15971E 00-,99452E 00 ,17780E 00-,97815E 00 ,22637E 00 238 4 51 2844
-,951106E 00 ,28679E 00-,91354E 00 ,32939E 00-,86602E 00 ,32671E 00 238 4 51 2845
-,809026E 00 ,28590E 00-,74314E 00 ,23637E 00-,66913E 00 ,22634E 00 238 4 51 2846
-,587786E 00 ,27186E 00-,50000E 00 ,33777E 00-,40674E 00 ,36359E 00 238 4 51 2847
-,309026E 00 ,32083E 00-,20791E 00 ,25054E 00-,10453E 00 ,23625E 00 238 4 51 2848
 ,132696E-05 ,34217E 00 ,10453E 00 ,53032E 00 ,20791E 00 ,69295E 00 238 4 51 2849
 ,309026E 00 ,72599E 00 ,40674E 00 ,62039E 00 ,50000E 00 ,47962E 00 238 4 51 2850
 ,587796E 00 ,44544E 00 ,66913E 00 ,58985E 00 ,74315E 00 ,86043E 00 238 4 51 2851
 ,809026E 00 ,11205E 01 ,86603E 00 ,12473E 01 ,91355E 00 ,12076E 01 238 4 51 2852
 ,951106E 00 ,10597E 01 ,97815E 00 ,89499E 00 ,99452E 00 ,77990E 00 238 4 51 2853
 ,100000E 01 ,74019E 00 ,00000E 00 ,00000E 00 ,00000E 00 ,00000E 00 238 4 51 2854
 0,0     + 0 0,10    + 8            0              0              1            31 238 4 51 2855
           31            2            0              0              0             0 238 4 51 2856
-,100000E 01 ,14440E-01-,99452E 00 ,26595E-01-,97815E 00 ,76177E-01 238 4 51 2857
-,951106E 00 ,16538E 00-,91354E 00 ,24117E 00-,86602E 00 ,23722E 00 238 4 51 2858
-,809026E 00 ,16283E 00-,74314E 00 ,10617E 00-,66913E 00 ,13617E 00 238 4 51 2859
-,587786E 00 ,21090E 00-,50000E 00 ,23739E 00-,40674E 00 ,20603E 00 238 4 51 2860
-,309026E 00 ,19724E 00-,20791E 00 ,26327E 00-,10453E 00 ,34567E 00 238 4 51 2861
 ,132696E-05 ,35965E 00 ,10453E 00 ,33340E 00 ,20791E 00 ,39971E 00 238 4 51 2862
```

```
 ,30902E 00 ,57299E 00 ,40674E 00 ,74349E 00 ,50000E 00 ,74111E 00 238 4 51 2863
 ,50779E 00 ,61687E 00 ,66913E 00 ,63308E 00 ,74315E 00 ,97464E 00 238 4 51 2864
 ,80902E 00 ,14965E 01 ,86603E 00 ,18232E 01 ,91355E 00 ,17073E 01 238 4 51 2865
 ,95106E 00 ,12489E 01 ,97815E 00 ,75421E 00 ,99452E 00 ,44307E 00 238 4 51 2866
 ,10000E 01 ,34714E 00 ,00000E 00 ,00000E 00 ,00000E 00 ,00000E 00 238 4 51 2867
 0,0     + 0 0,20    + 6          0           0           1           31 238 4 51 2868
           31            2          0           0           0            0 238 4 51 2869
-,10000E 01 ,89030E-01-,99452E 00 ,10205E 00-,97815E 00 ,13610E 00 238 4 51 2870
-,95106E 00 ,17015E 00-,91354E 00 ,17221E 00-,86602E 00 ,13295E 00 238 4 51 2871
-,80902E 00 ,65949E-01-,74314E 00 ,73603E-01-,66913E 00 ,96870E-01 238 4 51 2872
-,50778E 00 ,11909E 00-,50000E 00 ,11816E 00-,40674E 00 ,11265E 00 238 4 51 2873
-,30902E 00 ,13022E 00-,20791E 00 ,16878E 00-,10453E 00 ,20295E 00 238 4 51 2874
 ,13269E-05 ,22131E 00 ,10453E 00 ,24521E 00 ,20791E 00 ,30608E 00 238 4 51 2875
 ,30902E 00 ,40438E 00 ,40674E 00 ,50082E 00 ,50000E 00 ,56929E 00 238 4 51 2876
 ,50779E 00 ,65869E 00 ,66913E 00 ,65539E 00 ,74315E 00 ,11470E 01 238 4 51 2877
 ,80902E 00 ,13804E 01 ,86603E 00 ,14686E 01 ,91355E 00 ,16476E 01 238 4 51 2878
 ,95106E 00 ,23624E 01 ,97815E 00 ,37410E 01 ,99452E 00 ,52151E 01 238 4 51 2879
 ,10000E 01 ,58584E 01 ,00000E 00 ,00000E 00 ,00000E 00 ,00000E 00 238 4 51 2880

 9,22380+ 4 2,36006+ 2          0           2           0            0 238 4  0 2881
 0,0     + 0 2,36006+ 2          0           2           0            0 238 4 52 2882
 0,0     + 0 0,0     + 0         0           0           1            6 238 4 52 2883
               6                 2           0           0            0 238 4 52 2884
 0,0     + 0 ,146620+ 6          0           0           1            2 238 4 52 2885
               2                 2           0           0            0 238 4 52 2886
-1,0     + 0 0,5     + 0 1,0     + 0 0,5     + 0 0,0     + 0 0,0      + 0 238 4 52 2887
 0,0     + 0 ,15     + 7          0           0           1           31 238 4 52 2888
              31                 2           0           0            0 238 4 52 2889
-,10000E 01 ,33688E 00-,99452E 00 ,33860E 00-,97815E 00 ,34356E 00 238 4 52 2890
-,95106E 00 ,35121E 00-,91354E 00 ,36092E 00-,86602E 00 ,37236E 00 238 4 52 2891
-,80902E 00 ,38565E 00-,74314E 00 ,40136E 00-,66913E 00 ,42015E 00 238 4 52 2892
-,50778E 00 ,44255E 00-,50000E 00 ,46827E 00-,40674E 00 ,49608E 00 238 4 52 2893
-,30902E 00 ,52377E 00-,20791E 00 ,54860E 00-,10453E 00 ,56784E 00 238 4 52 2894
 ,13269E-05 ,57949E 00 ,10453E 00 ,58276E 00 ,20791E 00 ,57822E 00 238 4 52 2895
 ,30902E 00 ,56764E 00 ,40674E 00 ,55545E 00 ,50000E 00 ,53504E 00 238 4 52 2896
 ,50779E 00 ,52326E 00 ,66913E 00 ,51004E 00 ,74315E 00 ,49642E 00 238 4 52 2897
 ,80902E 00 ,48791E 00 ,86603E 00 ,47792E 00 ,91355E 00 ,46619E 00 238 4 52 2898
 ,95106E 00 ,45906E 00 ,97815E 00 ,45137E 00 ,99452E 00 ,44618E 00 238 4 52 2899
 ,10000E 01 ,44433E 00 ,00000E 00 ,00000E 00 ,00000E 00 ,00000E 00 238 4 52 2900
 0,0     + 0 ,30     + 7          0           0           1           31 238 4 52 2901
              31                 2           0           0            0 238 4 52 2902
-,10000E 01 ,63620E-01-,99452E 00 ,64741E-01-,97815E 00 ,67972E-01 238 4 52 2903
-,95106E 00 ,73135E-01-,91354E 00 ,80532E-01-,86602E 00 ,91504E-01 238 4 52 2904
-,80902E 00 ,10858E 00-,74314E 00 ,13506E 00-,66913E 00 ,17402E 00 238 4 52 2905
-,50778E 00 ,22699E 00-,50000E 00 ,29286E 00-,40674E 00 ,36740E 00 238 4 52 2906
-,30902E 00 ,44383E 00-,20791E 00 ,51420E 00-,10453E 00 ,57162E 00 238 4 52 2907
 ,13269E-05 ,61166E 00 ,10453E 00 ,63406E 00 ,20791E 00 ,64262E 00 238 4 52 2908
 ,30902E 00 ,64394E 00 ,40674E 00 ,64553E 00 ,50000E 00 ,65359E 00 238 4 52 2909
 ,50779E 00 ,67126E 00 ,66913E 00 ,69795E 00 ,74315E 00 ,72996E 00 238 4 52 2910
 ,80902E 00 ,76195E 00 ,86603E 00 ,76889E 00 ,91355E 00 ,80768E 00 238 4 52 2911
 ,95106E 00 ,81794E 00 ,97815E 00 ,82165E 00 ,99452E 00 ,82199E 00 238 4 52 2912
 ,10000E 01 ,82174E 00 ,00000E 00 ,00000E 00 ,00000E 00 ,00000E 00 238 4 52 2913
 0,0     + 0 ,60     + 7          0           0           1           31 238 4 52 2914
              31                 2           0           0            0 238 4 52 2915
-,10000E 01 ,18726E-01-,99452E 00 ,22893E-01-,97815E 00 ,34285E-01 238 4 52 2916
-,95106E 00 ,53352E-01-,91354E 00 ,87702E-01-,86602E 00 ,14920E 00 238 4 52 2917
-,80902E 00 ,24074E 00-,74314E 00 ,34419E 00-,66913E 00 ,42404E 00 238 4 52 2918
-,50778E 00 ,44930E 00-,50000E 00 ,41780E 00-,40674E 00 ,36200E 00 238 4 52 2919
-,30902E 00 ,32632E 00-,20791E 00 ,34482E 00-,10453E 00 ,40257E 00 238 4 52 2920
 ,13269E-05 ,46572E 00 ,10453E 00 ,50158E 00 ,20791E 00 ,50607E 00 238 4 52 2921
```

```
 ,36902E 00 ,50475E 00 ,40674E 00 ,53083E 00 ,50000E 00 ,59945E 00 238 4 52 2923
 ,56779E 00 ,69830E 00 ,66913E 00 ,79871E 00 ,74315E 00 ,87523E 00 238 4 52 2924
 ,80902E 00 ,91758E 00 ,86603E 00 ,92937E 00 ,91355E 00 ,91966E 00 238 4 52 2925
 ,95106E 00 ,89716E 00 ,97815E 00 ,87013E 00 ,99452E 00 ,84791E 00 238 4 52 2926
 ,10000E 01 ,83926E 00 ,00000E 00 ,00000E 00 ,00000E 00 ,00000E 00 238 4 52 2927
 0.0    + 0 .10    + 8           0           0           1          31 238 4 52 2928
         31           2           0           0           0           0 238 4 52 2929
-,10000E 01 ,77642E-01-,99452E 00 ,73892E-01-,97815E 00 ,74329E-01 238 4 52 2930
-,95106E 00 ,97285E-01-,91354E 00 ,14538E 00-,86602E 00 ,19797E 00 238 4 52 2931
-,80902E 00 ,24831E 00-,74314E 00 ,28421E 00-,66913E 00 ,29041E 00 238 4 52 2932
-,58778E 00 ,26148E 00-,50000E 00 ,22507E 00-,40674E 00 ,22493E 00 238 4 52 2933
-,30902E 00 ,26802E 00-,20791E 00 ,31010E 00-,10453E 00 ,31585E 00 238 4 52 2934
 ,13269E-05 ,31624E 00 ,10453E 00 ,37184E 00 ,20791E 00 ,48132E 00 238 4 52 2935
 ,30902E 00 ,56785E 00 ,40674E 00 ,57688E 00 ,50000E 00 ,56943E 00 238 4 52 2936
 ,58779E 00 ,64608E 00 ,66913E 00 ,83536E 00 ,74315E 00 ,10476E 01 238 4 52 2937
 ,80902E 00 ,11818E 01 ,86603E 00 ,12341E 01 ,91355E 00 ,12787E 01 238 4 52 2938
 ,95106E 00 ,13667E 01 ,97815E 00 ,14775E 01 ,99452E 00 ,15616E 01 238 4 52 2939
 ,10000E 01 ,15913E 01 ,00000E 00 ,00000E 00 ,00000E 00 ,00000E 00 238 4 52 2940
 0.0    + 0 ,20    + 6           0           0           1          31 238 4 52 2941
         31           2           0           0           0           0 238 4 52 2942
-,10000E 01 ,32854E-01-,99452E 00 ,53218E-01-,97815E 00 ,10310E 00 238 4 52 2943
-,95106E 00 ,16703E 00-,91354E 00 ,23940E 00-,86602E 00 ,30020E 00 238 4 52 2944
-,80902E 00 ,30706E 00-,74314E 00 ,24700E 00-,66913E 00 ,17379E 00 238 4 52 2945
-,58778E 00 ,15208E 00-,50000E 00 ,18075E 00-,40674E 00 ,20325E 00 238 4 52 2946
-,30902E 00 ,19886E 00-,20791E 00 ,19911E 00-,10453E 00 ,22427E 00 238 4 52 2947
 ,13269E-05 ,25328E 00 ,10453E 00 ,27271E 00 ,20791E 00 ,30519E 00 238 4 52 2948
 ,30902E 00 ,36461E 00 ,40674E 00 ,42806E 00 ,50000E 00 ,48532E 00 238 4 52 2949
 ,58779E 00 ,57673E 00 ,66913E 00 ,74302E 00 ,74315E 00 ,97433E 00 238 4 52 2950
 ,80902E 00 ,12535E 01 ,86603E 00 ,16077E 01 ,91355E 00 ,20466E 01 238 4 52 2951
 ,95106E 00 ,24709E 01 ,97815E 00 ,27349E 01 ,99452E 00 ,28111E 01 238 4 52 2952
 ,10000E 01 ,26110E 01 ,00000E 00 ,00000E 00 ,00000E 00 ,00000E 00 238 4 52 2953
                                                                    238 4  0 2954
```

Fig. 1.

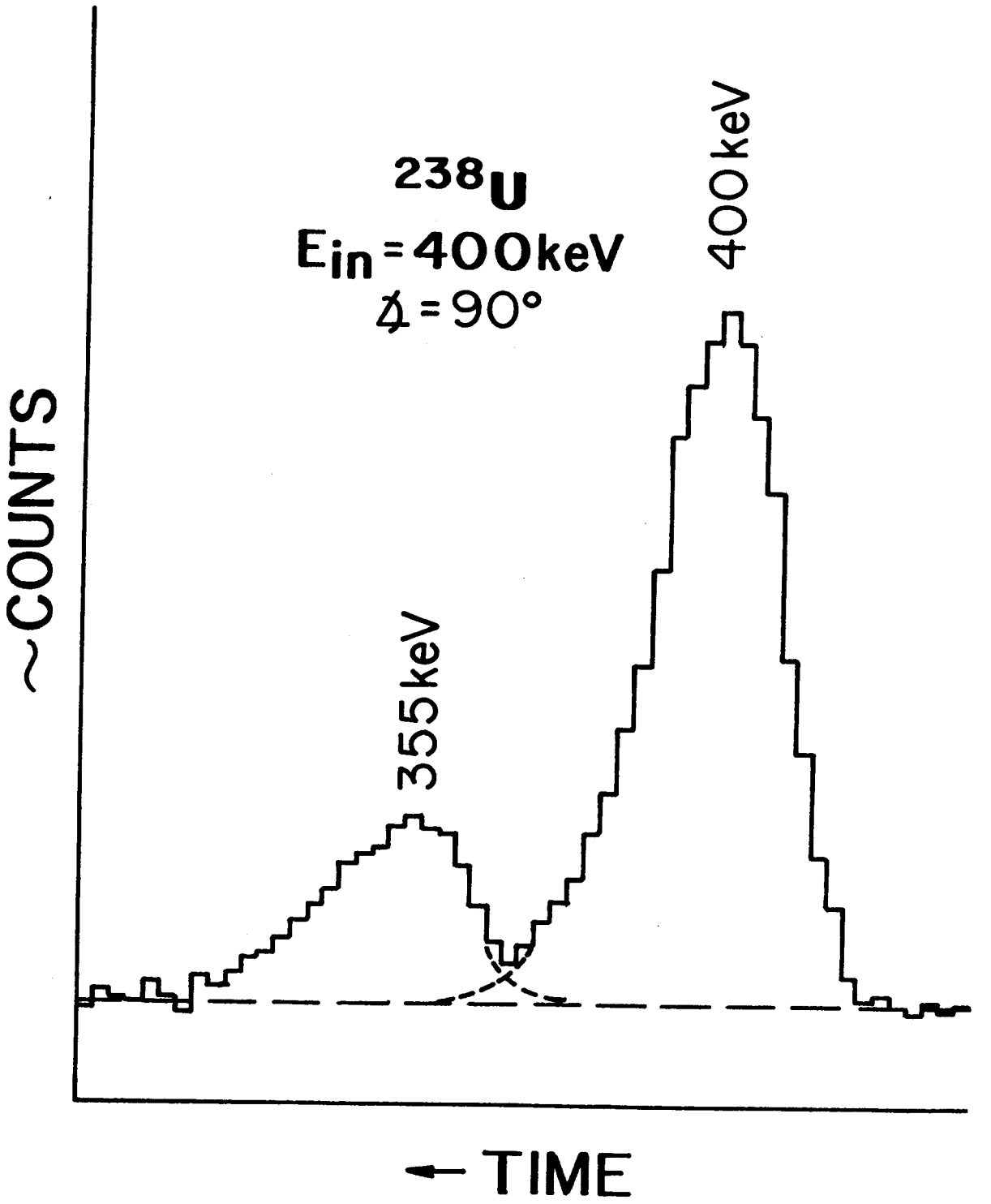

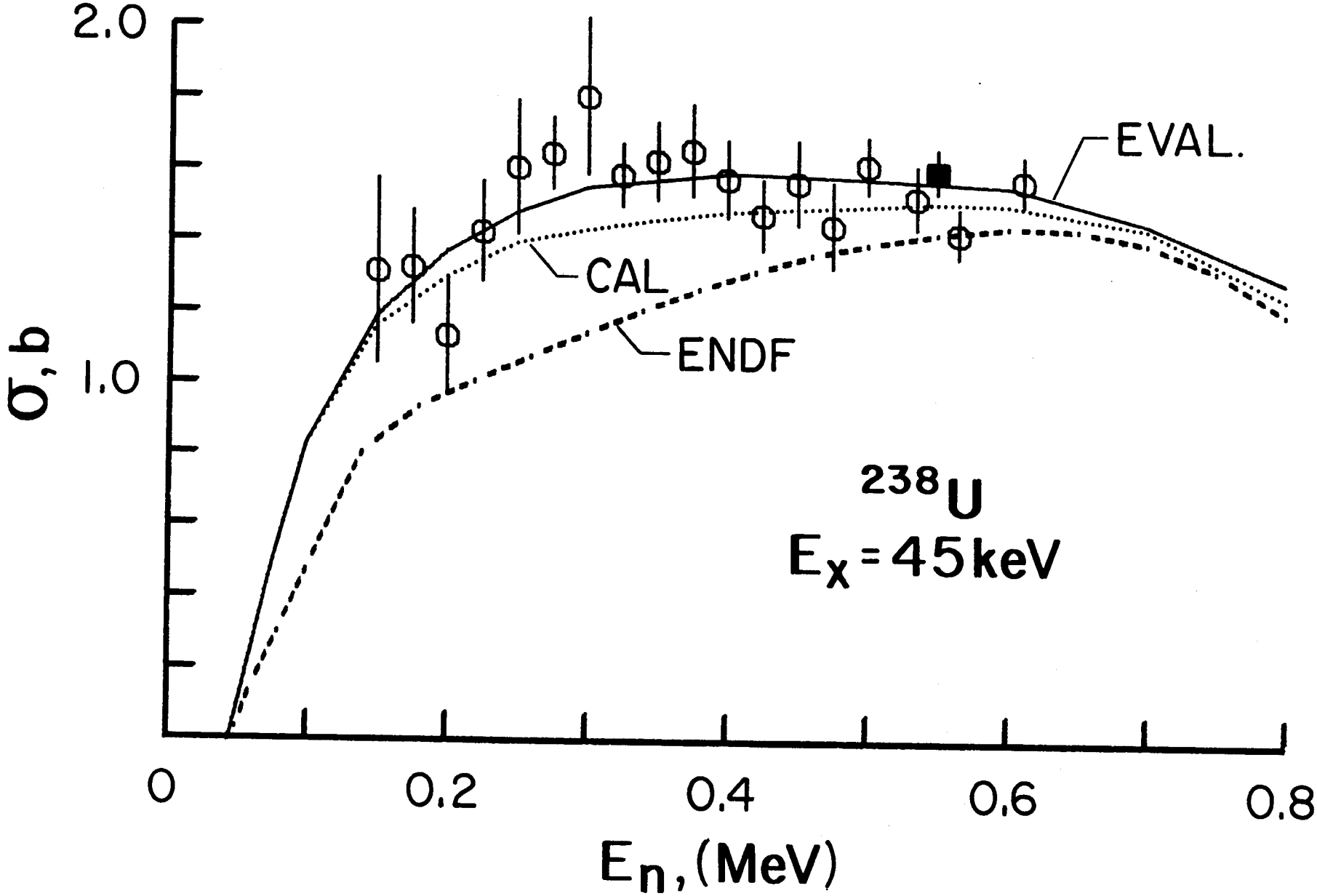

Fig. 2.

Fig. 3.

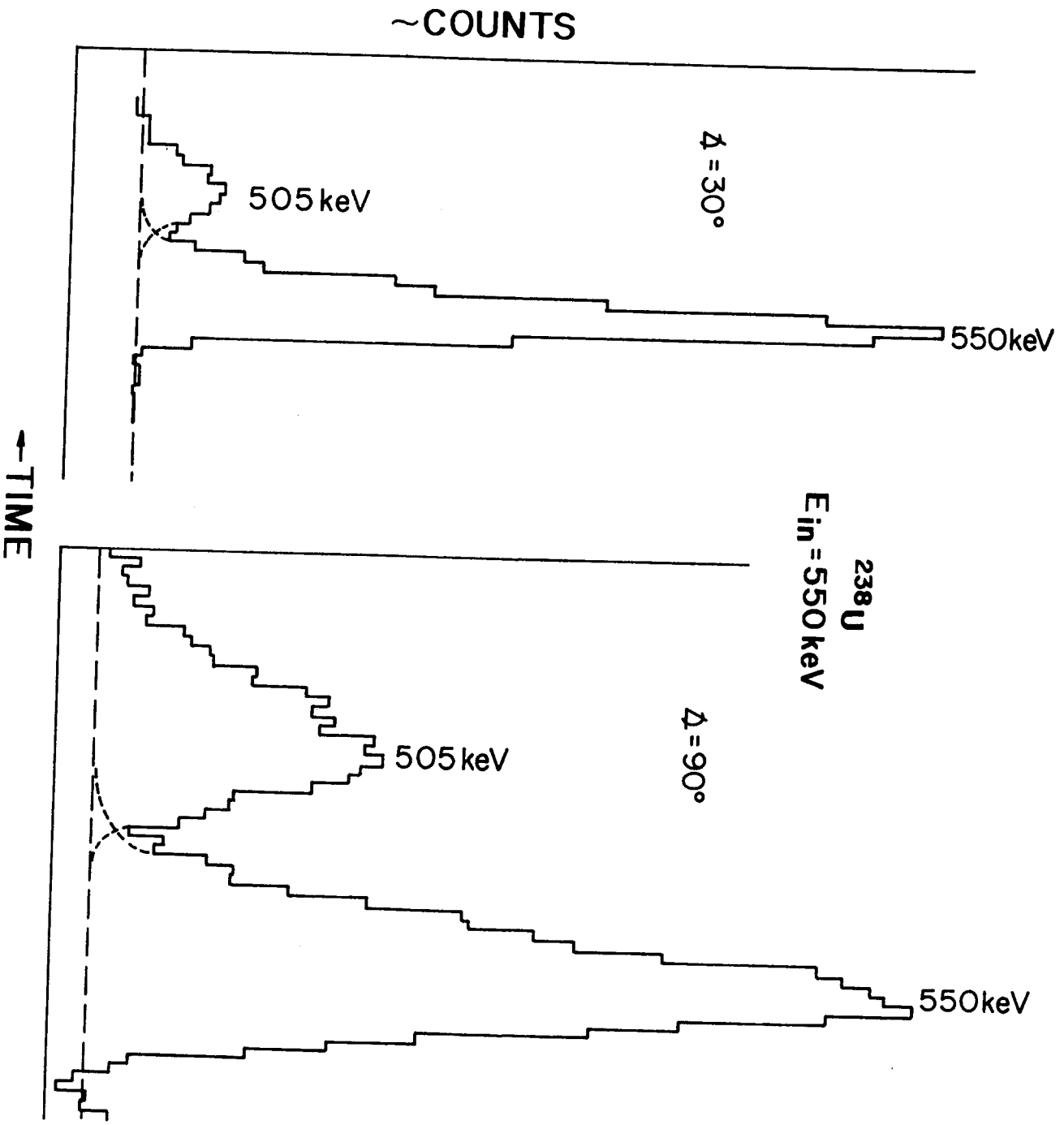
~COUNTS
505keV
Δ=30°
550keV
←TIME
238U
Ein=550keV
505keV
Δ=90°
550keV

Fig. 4.

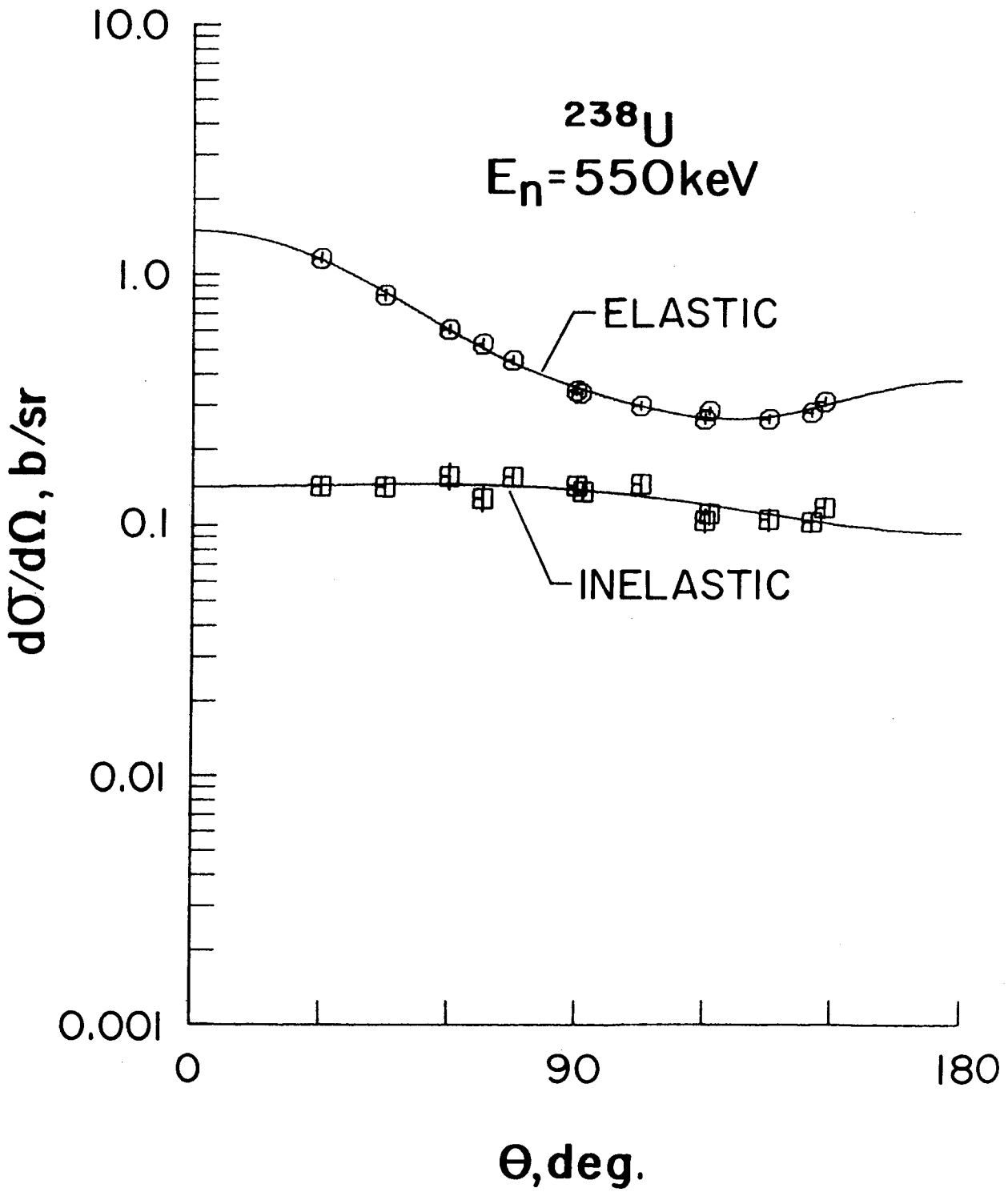
10.0
1.0
0.1
0.01
0.001
0
90
180
238U
En=550keV
ELASTIC
INELASTIC
dσ/dΩ, b/sr
θ,deg.

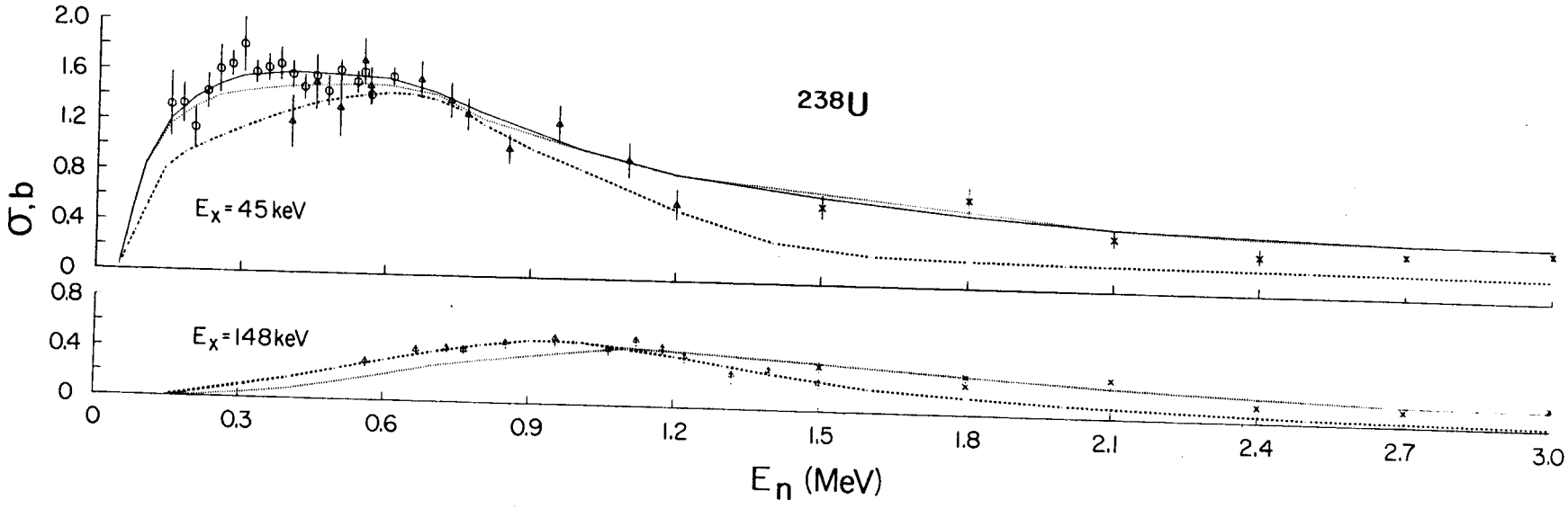
238U
Ex = 45 keV
Ex = 148 keV
σ, b
En (MeV)
2.0
1.6
1.2
0.8
0.4
0
0.3
0.6
0.9
1.2
1.5
1.8
2.1
2.4
2.7
3.0

Fig. 5.

Fig. 6.

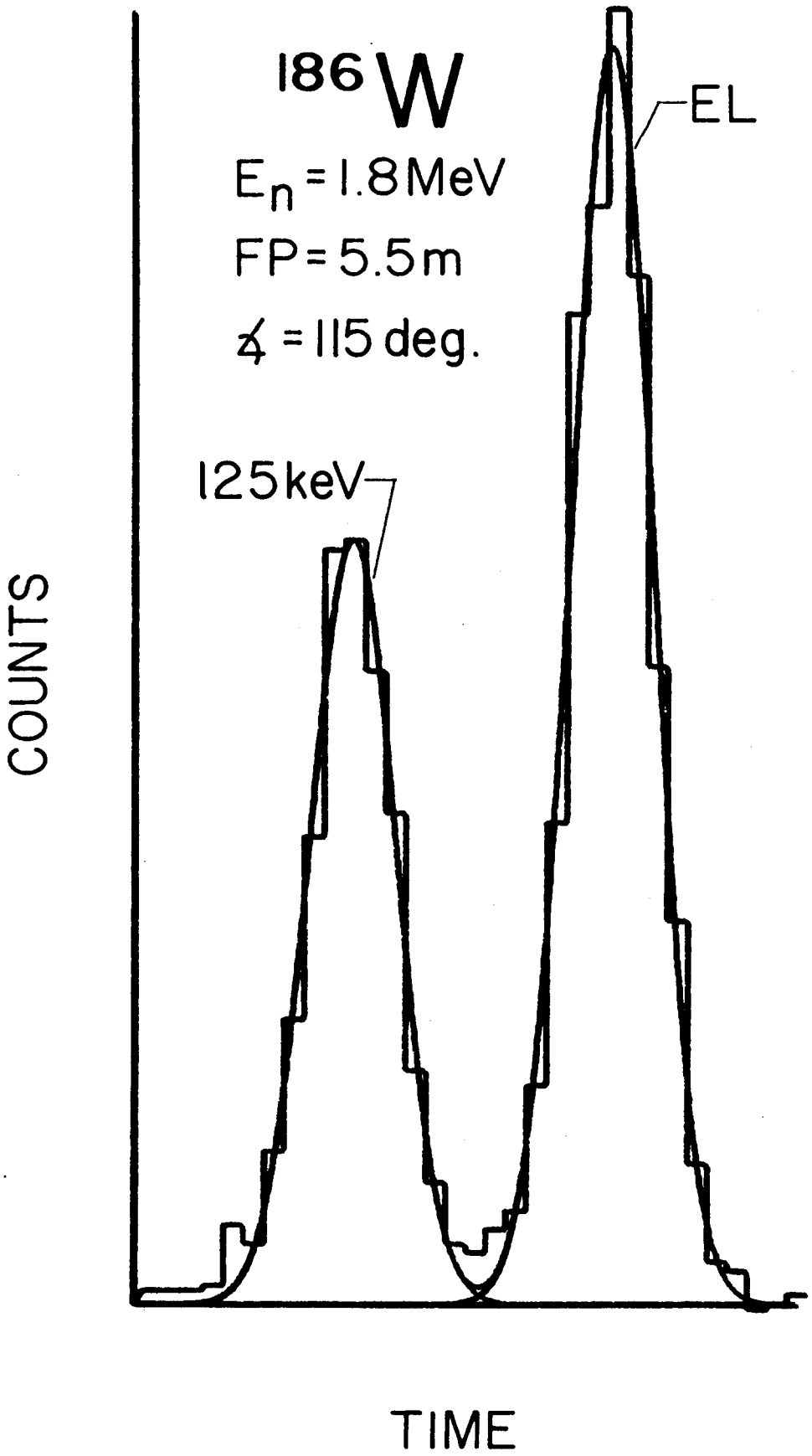

Fig. 7.

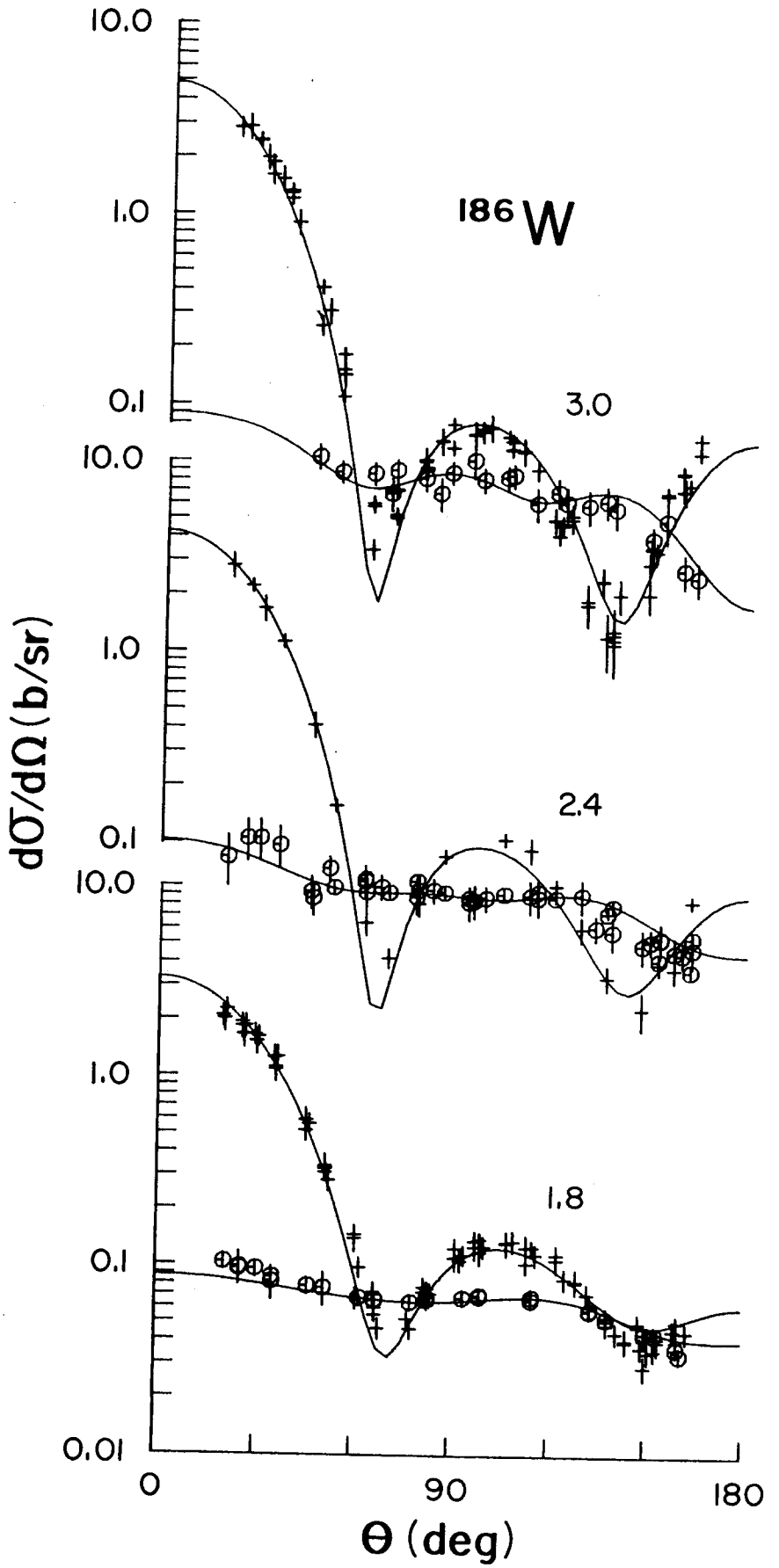
10.0
1.0
0.1
186W
3.0
10.0
1.0
0.1
2.4
10.0
1.0
0.1
1.8
0.01
dσ/dΩ (b/sr)
0
90
180
Θ (deg)

Fig. 8.

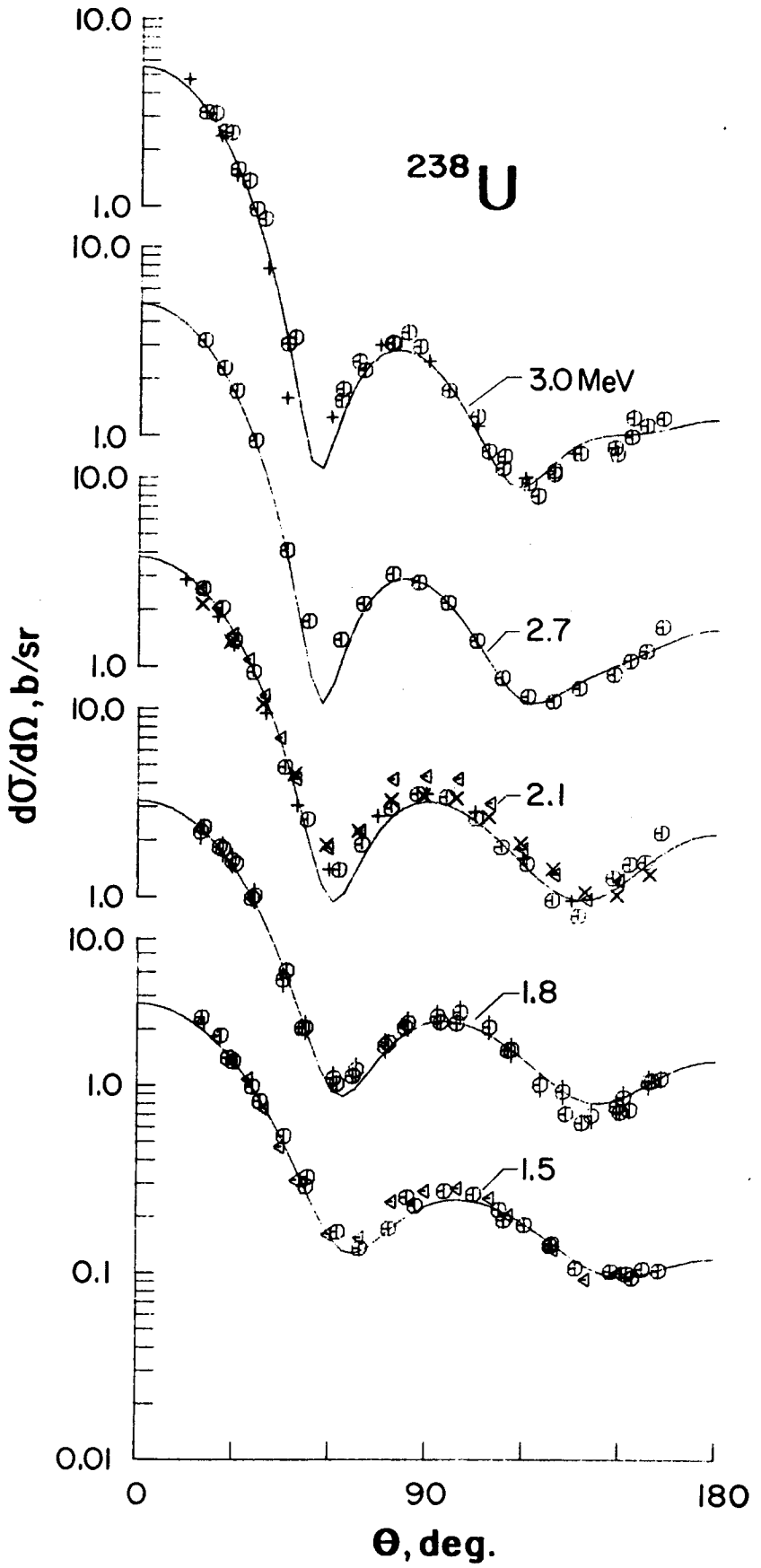

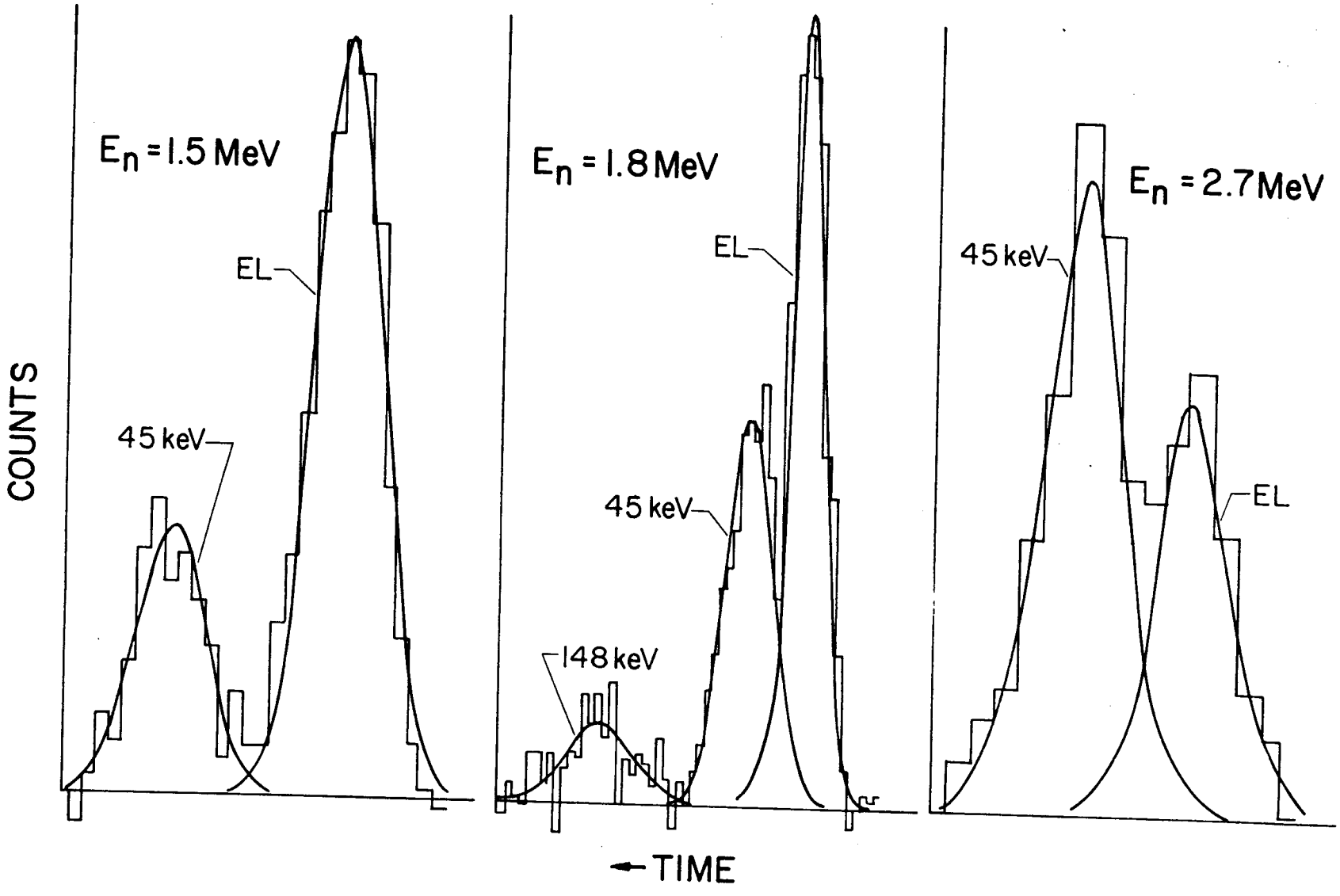
E_n = 1.5 MeV
EL
45 keV
E_n = 1.8 MeV
EL
45 keV
148 keV
E_n = 2.7 MeV
45 keV
EL
COUNTS
TIME

Fig. 9.

Fig. 10.

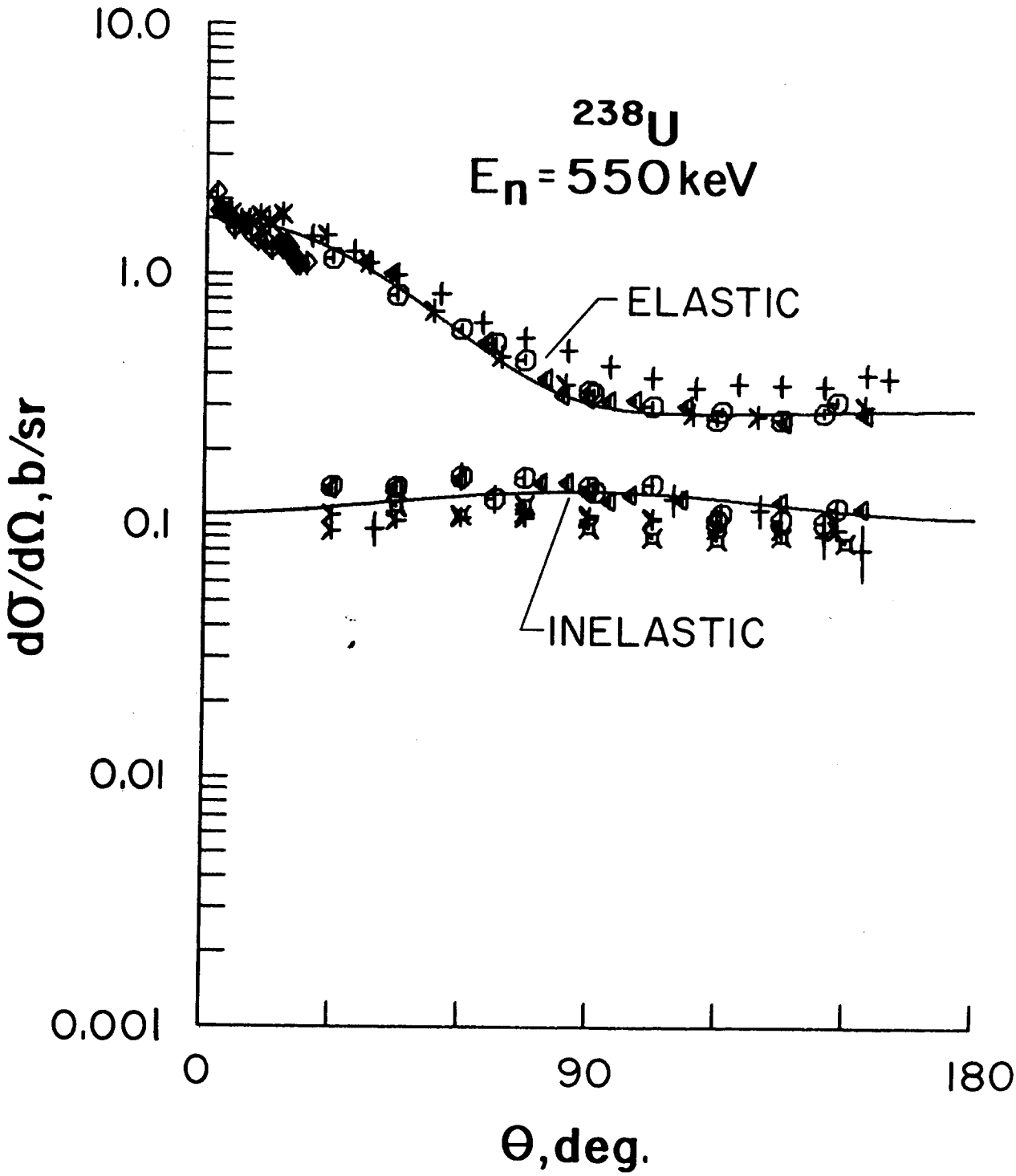
10.0
1.0
0.1
0.01
0.001
0
90
180
dσ/dΩ, b/sr
θ, deg.
238U
En = 550 keV
ELASTIC
INELASTIC

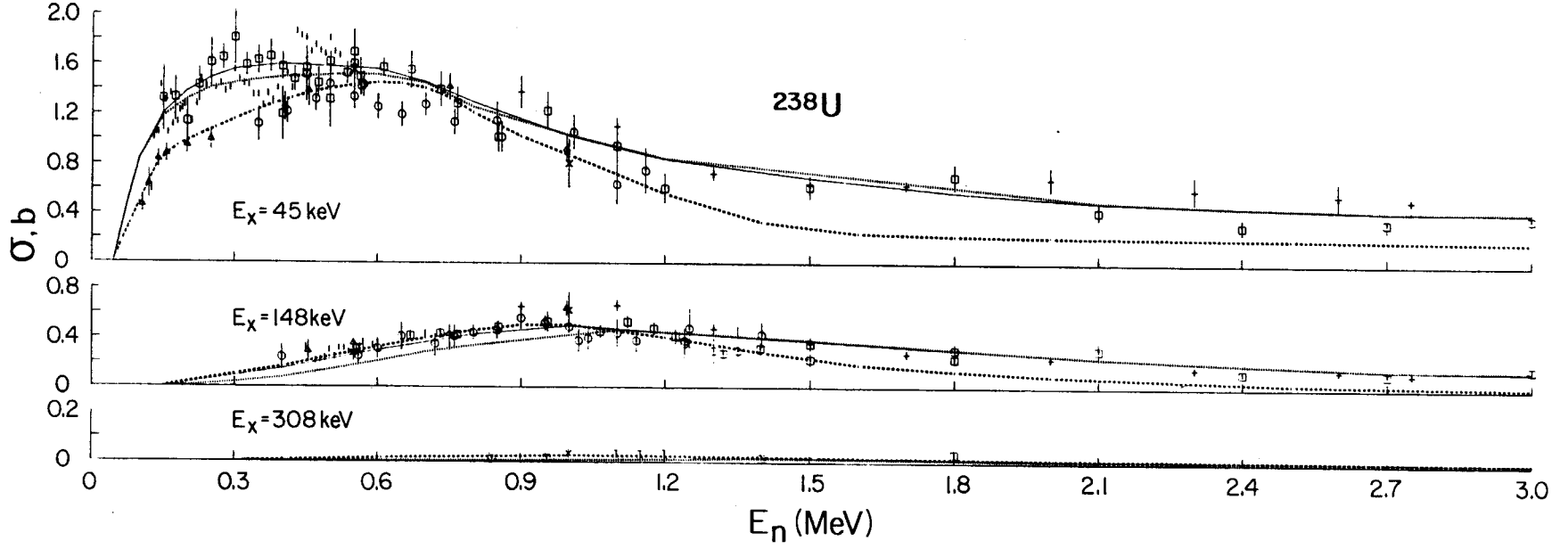
238U
Ex = 45 keV
Ex = 148keV
Ex = 308 keV
σ, b
En (MeV)
2.0
1.6
1.2
0.8
0.4
0
0.8
0.4
0
0.2
0
0
0.3
0.6
0.9
1.2
1.5
1.8
2.1
2.4
2.7
3.0

Fig. 11.